Learning to learn persistently modifies a neocortical-hippocampal excitatory-inhibitory subcircuit

Ain Chung[1], Claudia Garcia Jou[2], Dino Dvorak[1], Nida Hussain[1], André A. Fenton[1,3,4]

[1]Center for Neural Science, New York University
[2]Department of Biological Sciences, City University of New York, Hunter College
[3]Neuroscience Institute at the NYU Langone Medical Center
[4]Robert F. Furchgott Center Neural and Behavioral Science, Department of Physiology and Pharmacology, State University of New York, Downstate Medical Center

Address for correspondence:

André Fenton, Neurobiology of Cognition Laboratory, Center for Neural Science, New York University, 4 Washington Place, Room 980. Email: afenton@nyu.edu

Acknowledgements:

Supported by NIH grants R01MH115304, R01NS105472, and R01AG043688. We are grateful to Dr. Todd Sacktor for the gift of the PKMζ antibody.

Data Availability:

The datasets generated during and/or analysed during the current study are available from the corresponding author on reasonable request.

Code Availability:

The custom Matlab code used to perform analyses in this study are available at: https://github.com/FentonLab/Chung_etal_LearningToLearnCode.git

SUMMARY

The neurobiology of psychological concepts like schema, and psychotherapeutic strategies of cognitive behavioral therapy (CBT) is poorly understood, partly because learning to process information confounds, and is rarely distinguished from acquiring content-specific memory. Learning to learn changes one's overall information-processing ability, whereas neurobiological investigations typically focus on memory for content from particular experiences. We investigated entorhinal cortex-to-dentate gyrus neural circuit changes while mice learn to learn during cognitive control training (CCT) to judiciously use and ignore information. CCT changes synaptic circuit function by persistently modifying an excitatory-inhibitory interneuron subcircuit lasting weeks. CCT increases dentate gyrus expression of PKMζ that maintains long-term potentiation, particularly in somatostatin-expressing inhibitory interneurons that mediate both widespread inhibition, and through disinhibition, also local excitation of dentate gyrus. These findings that CCT modifies excitation-inhibition circuit coordination provide direct neurobiological evidence for a CBT-neuroplasticity hypothesis that, beyond particular item/event associations, learning to learn persistently changes neural circuit function.

Neurobiological investigations of learning typically focus on the acquisition of memory for content-specific information, whereas outside the laboratory, a particular memory is often acquired concurrently with learning to learn that general class of information. Learning to learn relies on acquiring cognitive skills, forming so-called schema, a cognitive framework for memory information processing that is abstracted from the particular content of memory [1,2] and can be the basis of a particular mindset that directs future learning and experience [3]. Learning to learn is the basis of the cognitive behavioral therapist's effort to improve subsequent understanding, learning and overall function of their patients. While it is tempting to conjecture that the cognitive psychology of schema, the psychotherapeutic practice of cognitive behavioral therapy (CBT),

and the neurobiology of memory and neural information processing are intimately related, the nature of those relations are speculative. The dominant CBT-neuroplasticity hypothesis asserts that CBT causes neural plasticity to change brain function, but beyond changes in sensory systems [4,5], there is scant evidence for the three key predictions of 1) CBT-induced 2) long-lasting, and 3) memory-nonspecific training-induced changes in neural circuit function.

Here, we test these predictions of the CBT-neuroplasticity hypothesis using freely-behaving mice. We exploited an experimental platform that demonstrated persistent *ex vivo* and anesthetized *in vivo* electrophysiological changes in GABAergic-sensitive hippocampus synaptic function after learning an active place avoidance task [6]. The task requires intact hippocampal activity [7,8], and persistent PKMzeta (PKMζ)-mediated long-term potentiation (LTP) of hippocampal synaptic function [9-11]. Hippocampus place cell discharge during the task mirrors ongoing performance as well as cognitive control of switching between task relevant and irrelevant information, demonstrating representational multi-tasking [12-14]. Furthermore, resembling effective CBT, preemptive training is sufficient to prevent subsequent neuropsychiatric-related cognitive impairments in a neurodevelopmental rat model [15].

We began by investigating whether cognitive control training causes learning to learn in C57Bl6 mice by comparing performance during initial training and subsequent training in a novel environment (Fig. 1A). Mice were initially trained to perform one of three task variants. The cognitive control training (CCT) group was trained in the R+A- active place avoidance task variant that is predicted to cause learning to learn. Mice on a rotating (1 rpm) arena learn the room-based location of a stationary shock zone, and must ignore the arena-based, unpredictable locations where they experience shock [16], although hippocampus discharge represents these places [12,13]. Mice in the place learning (PL) control group were trained in the R+ task variant that differs from the R+A- task variant by the presence of shallow water on the

arena surface [16]. The water attenuates the olfactory cues used for recognizing places on the arena, so R+ training requires less cognitive control to ignore the task-irrelevant arena locations of shock, and is not expected to cause learning to learn. The spatial exploration (SE) group experienced the identical physical conditions as the CCT mice, but shock was never turned on so they are also not expected to demonstrate learning to learn. After initial training, all mice were subsequently trained in a novel environment to do the same R+A- task that requires cognitive control (Fig. 1A).

Pretraining, Initial and Subsequent Learning

The three groups differ in the initial but not the subsequent pretraining trials with no shock, because in the shallow water the mice walk less (Group x Trial two-way RM ANOVA; n's=10; group: $F_{2,26} = 15.0$, $p = 10^{-5}$; Trial: $F_{1,51.6} = 4.64$, $p = 0.04$; interaction: $F_{2,51.6} = 4.07$, $p = 0.02$; PL during initial < all other group x trials measures). This resulted in group differences in the number of times the mice enter the location of the future shock zone (Group: $F_{2,26} = 6.71$, $p = 0.0045$, Trial: $F_{2,51.1} = 0.60$, $p = 0.44$; interaction: $F_{1,51.1} = 1.55$, $p = 0.22$; PL < CCT = SE), as can be seen in Fig. 1B. Consequently, performance in the initial and subsequent training sessions is analyzed separately.

During initial training the groups continued to differ in how much they walked, but this time because the animals that experienced shock walk less and restrict themselves to the arena periphery; the conditioned mice did not differ (Group x Trial two-way RM ANOVA, Group: $F_{2,25} = 19.54$, $p = 10^{-6}$, Tukey-HSD: SE > CCT = PL). Place avoidance learning measured as decreasing errors, i.e. entrances into the shock zone was robust with significant effects of Group and the Group X Trial interaction (Group: $F_{2,25} = 67.5$, $p = 10^{-11}$, Tukey-HSD: SE > CCT = PL; Interaction: $F_{4,51.4} = 4.15$, $p = 0.006$). The two conditioned groups showed similar learning

(Group: $F_{1,19.1} = 0.0004$, $p = 0.98$; Trial: $F_{2,33} = 12.92$, $p = 10^{-5}$, Tukey-HSD Trial1 > Trial 2 > Trial 3; Interaction: $F_{2,33} = 0.33$, $p = 0.7$). One-week memory retention was robust with an obvious effect of Group measured by entrances into the shock zone ($F_{2,26} = 80.0$, $p = 10^{-12}$, Tukey-HSD: SE > CCT = PL) as well as the time to first enter the shock zone in the two conditioned groups with PL better than CCT (Group: $F_{1,20} = 6.98$, $p = 0.02$).

During subsequent training in a novel environment, all mice first received pretraining on a rotating arena without shock, followed by identical R+A- cognitive control training with shock. During pretraining, the mice did not express thigmotaxis or avoidance as described above, confirming mice treat the environment as novel (Fig. 1B). The groups did not differ in how much they walked during the training trials (Group: $F_{2,26} = 0.47$, $p = 0.6$; Trials: $F_{2,25} = 0.98$, $p = 0.4$; Interaction: $F_{4,29.2} = 0.65$, $p = 0.6$). All mice learned the new R+A- place avoidance rapidly and when assessed across the 30-min trials, the groups could not be distinguished by errors (Group: $F_{2,26} = 0.11$; $p = 0.9$; Trials: $F_{2,25} = 32.57$, $p = 10^{-7}$, Tukey-HSD: Ts1 > Ts2 = Ts3; Interaction; $F_{4,29.2} = 1.84$, $p = 0.15$), or by the time to first enter the shock zone (Group: $F_{2,26} = 0.51$; $p = 0.6$; Trials: $F_{2,25} = 33.29$, $p = 10^{-8}$, Tukey-HSD: Ts1 < Ts2 < Ts3; Interaction: $F_{4,29.2} = 0.61$, $p = 0.66$). Although there was a significant effect of group on the errors at the 1-week retention test with the PL group tending to make more errors, ($F_{2,24} = 3.86$, $p = 0.04$), Tukey-HSD post-hoc tests did not in fact distinguish the groups; nor were the groups different according to the time to first enter the shock zone ($F_{2,24} = 0.67$, $p = 0.5$), which is a strict measure of memory retention because it is not influenced by within-session reinforcement or learning.

Because learning may have been rapid, and effectively complete within the first 30 min, we examined avoidance across the six 5-min epochs of the first subsequent training trial (Ts1). The effect of the epochs was significant, indicating learning ($F_{5,130} = 43.09$, $p = 10^{-26}$) as was the Group X Epoch interaction ($F_{10,130} = 2.89$, $p = 10^{-3}$). Post-hoc tests confirmed that with the

exception of the PL group's first epoch, the number of entrances during all other 5-min epochs were significantly fewer than that of the SE group's first epoch and exposure to shock (Fig. 1C). This suggests that the CCT group learned to learn during initial training, and this was supported by a significant correlation between the strength of place avoidance at the end of initial training (trial RET) and the strength of place avoidance during subsequent training (trial Ts1; $n = 12$, $r = 0.57$, $p = 0.05$). We then examined this possibility by analysis of the time series of the first 5 errors (Fig. 1D). The CCT mice increased the time to enter the shock zone faster than the other groups, consistent with learning to learn. The groups differed significantly ($F_{2,75.9} = 6.76$, $p = 10^{-3}$) and necessarily, the effect of entrance number was significant ($F_{4,60.1} = 23.26$, $p = 10^{-11}$). Tukey-HSD tests confirmed that compared to the time of the first entrance, the CCT group had significantly and reliably increased the time to enter the shock zone by their third entrance, whereas the other two groups had not done so by their 5th entrance.

Learning to Learn

Finally, we confirmed that the CCT mice had indeed learned to learn during initial training by comparing the times of the first 5 entrances on the first trials of Initial and Subsequent CCT (Fig. 1E). The effect of training phase was significant ($F_{1,50} = 14.59$, $p = 10^{-4}$) as was the effect of entrance number ($F_{4,50} = 9.81$, $p = 10^{-3}$), but not the interaction ($F_{4,50} = 2.41$, $p = 0.06$). Analysis of the number of entrances during the six 5-min epochs of the initial and subsequent first training trials further confirms that CCT causes the mice to learn to learn (Fig. 1S1; Phase: $F_{1,60} = 6.61$, $p = 0.01$; Time: $F_{5,60} = 9.89$, $p = 10^{-4}$; Phase X Time interaction: $F_{5,60} = 1.81$, $p=0.12$).

CCT also improved subsequent learning of a left-right (L/R) discrimination task in a novel T-maze environment (Fig. 1F), the reversal of which is sensitive to hippocampus function [17]. Mice

that had received initial CCT and SE training learned the first L/R discrimination equally well, and they were also indistinguishable two hours later when the reinforcement was reversed to require cognitive control for distinguishing between the initial and current safe and punished arms. However, the mice that had received CCT performed better when the contingency was reversed again to increase the cognitive control demand (Group $F_{1,22} = 12.36$, $p = 0.002$; trial: $F_{2,42} = 3.161$ $p = 0.054$; interaction: $F_{2,44} = 1.573$, $p = 0.219$).

CCT persistently changes neural circuit function

We had confirmed that the dentate gyrus (DG) is crucial for expressing active place avoidance following CCT training by targeting bilateral muscimol inactivation to DG (Fig. 2S1). Accordingly, to assess whether CCT training modifies neocortical-hippocampus circuit function, a subset of the mice had been implanted with stimulating electrodes in the medial perforant path (MPP) entorhinal cortex input to DG and CA1 along with 32-site recording electrodes that spanned the somatodendritic axis of dorsal hippocampus (Fig. 2S2). We first confirmed electrode targeting of the MPP-DG connection using a transgenic mouse that predominantly expresses the inhibitory DREADD hM4Di in layer 2 of the medial entorhinal cortex (MEC) under control of the tTA-TetO system Fig 2S3; [18].

By measuring source-localized (Fig. 2S4) DG evoked potential responses to 0-250 μA test stimulation before and 2h after each training session, we evaluated whether the CCT, PL, and SE experiences change neocortical-hippocampus circuit function (Fig. 2A). The PL (n=5) and SE (n=5) training did not cause detectable changes, but initial CCT (n=5) reduced the source-localized fEPSP slope in the molecular layer of the suprapyramidal division of DG (supraDG; Fig. 2B); changes were minimal in the population spike and at the infrapyramidal division (infraDG), nor did electrode impedances or electrophysiological features such as the current

source density (CSD), or theta power change systematically (Fig. 2S5). CSD analysis shows that CCT reduces the current sink in the response at the inner molecular layer of supraDG, where the MPP preferentially terminates Fig. 2C; [19]. These changes were already observed 2 hours after the first CCT session and were maximal after the second trial (Fig. 2S6). When tested in a subset of 6 mice these CCT-induced functional changes persisted at least 60 days without further training (baseline > 7-d = 60-d experience: baseline vs. 7-d t_5=5.10; p = 0.004; baseline vs. 60-d t_5 = 4.42; p = 0.007).

Finally, to verify that these CCT-induced changes are not the direct result of the MPP stimulation, we took advantage of naturally occurring, highly-synchronous MPP activations known as type 2 dentate spikes, or as we will call them DS_M, which are distinct from type 1 dentate spikes (DS_L) that result from lateral perforant path (LPP) activation [20]. We reasoned that the DS_M responses should reflect the same changes that we observed from experimental MPP stimulation. As predicted, the slope of DS_M events decreased in the supraDG (Fig. 2S7). The DS_M did not change in the infraDG, mimicking the findings from experimental stimulation (Fig. 2C).

If the changes in neural circuit function caused by CCT are due to acquiring a content-specific place avoidance memory then learning an additional place avoidance should cause additional changes, whereas if the neural circuit changes result from the “process memory” of learning to learn [21] then the additional training should not cause incremental neural circuit changes. A new group of mice (n=5) received initial CCT and after the 1-week retention test, they received subsequent CCT to acquire a different place avoidance memory either in the same environment followed by CCT in a novel environment (n=2), or in counterbalanced order (n=3) to control for the sequence. Although subsequent learning was better than initial learning (Fig. 2S8), the

subsequent training experiences did not cause incremental changes in neural circuit function (Fig. 2D), consistent with process rather than content-specific memory.

CCT changes inhibitory circuit function

Having confirmed the three key predictions of the CBT-neuroplasticity hypothesis, we then investigated mechanisms of the attenuated synaptic response in supraDG. DG interneurons strongly regulate principal cell firing in freely-behaving rats [22]. CCT increases the sub-second coupling between action potential discharge of excitatory granule cells and inhibitory neurons in DG [12], and spatial learning increases DG mossy fiber-mediated feedforward inhibition [23], motivating us to hypothesize that CCT increases DG inhibition. Gad2Cre-ChR2-eYFP mice expressing the excitatory opsin in GABAergic neurons were used to test two predictions of this hypothesis (Fig. 3A; Fig. 3S1). Under urethane anesthesia that reduces ongoing activity (Fig. 3S1), light activation of Gad2+ DG cells in the vicinity of the recording site blocked population spike responses in all mice when light stimulation preceded MPP-stimulation by 5 ms indicating effectiveness of the inhibition and attenuation of potential feedback responses (Fig. 3S2). Importantly, activating this inhibition 5 ms before MPP stimulation (but not 0 ms before; Fig. 3S3), mimicked the CCT-induced attenuation of MPP responses at supraDG, whereas the attenuation was occluded when tested a week after CCT, but not after SE-training or in task-naïve mice (Fig. 3B). CCT also decreased inhibition at supraDG but not infraDG (Fig. 3S4) assessed with intact spiking by paired-pulse stimulation, whereas PL-training did not cause a decrease, all relative to task naïve mice. These findings suggest that CCT increases both inhibition and excitation-dependent disinhibition at supraDG but not infraDG (Fig. 3C,D).

We then exploited strongly reduced spontaneous activity in *ex vivo* hippocampus slices to test the possibility that CCT increases excitation-dependent inhibition. Optogenetic activation of

Gad2+ cells was used to induce inhibition at supraDG (Fig. 3E) but first we observed that fEPSP responses to MPP stimulation increase at supraDG (I-O AUC: $t_9 = 2.85$, $p = 0.02$) but not infraDG (I-O AUC: $t_{10} = 0.95$, $p = 0.36$) in *ex vivo* slices from Gad2Cre-ChR2-eYFP mice after CCT (Fig. 3F). This indicates CCT induces persistent synaptic potentiation, as reported for the Schaffer collateral synapse [4]. Paired-pulse MPP stimulation at short (< 10 ms) intervals also shows increased 5-ms latency inhibition at supraDG in the slices from CCT mice, but not long (> 20 ms) intervals, suggesting potentiated evoked inhibition selectively at supraDG (but not infraDG) of CCT mice (Fig, 3G; supraDG short intervals - group: $F_{1,10}=5.68$, $p = 0.04$; interval: $F_{3.15,31.49}=4.13$, $p = 0.01$; interaction: $F_{5,50}=0.95$, $p = 0.46$; supraDG long intervals - group: $F_{1,10}=0.16$, $p = 0.70$; interval: $F_{1.92,19.21}=7.62$, $p = 0.004$; interaction: $F_{3,30}=1.59$, $p = 0.21$; infraDG short intervals - group: $F_{1,10}=0.23$; $p = 0.64$; interval: $F_{1.97,19.69}=7.21$, $p = 0.005$; interaction: $F_{5,50}=0.34$, $p = 0.89$; infraDG long intervals - group: $F_{1,10}=0.004$; $p = 0.94$; interval: $F_{2.56,22.57}=0.05$, $p = 0.96$; interaction: $F_{3,30}=0.89$, $p = 0.46$). Activating channelrhodopsin in Gad2+ cells was then used to directly test whether CCT persistently increases disinhibition. Light activation 2 ms and 5 ms before, but not 10 ms before MPP stimulation caused increased supraDG synaptic population responses in slices from CCT mice but not from SE-trained mice, demonstrating increased disinhibition after CCT (Fig. 3H,I; supraDG - group: $F_{1,6}=3.37$; $p = 0.12$; interval: $F_{2.04,12.26}=1.75$, $p=0.21$; interaction: $F_{7,42}=1.29$, $p=0.28$). Together these findings indicate that CCT increases synaptic potentiation (Fig. 3F) as well as both feedback inhibition (Fig. 3G) and disinhibition (Fig. 3I) that together produce a global attenuation of the synaptic response to MPP activation observed in the awake mouse (Fig. 2).

CCT increases PKMζ in dentate gyrus and a subclass of hilar interneurons

Finally, we investigated a potential inhibitory interneuron subcircuit that could mediate both feedforward inhibition and disinhibition of MPP inputs (Fig. 3J). A candidate subcircuit is

comprised of GABAergic HIPP (hilar perforant path projecting) interneurons that mediate inhibition onto granule cells as well as onto various inhibitory cells that provide perforant path-mediated feedforward inhibition of granule cell dendrites [24,25]. HIPP cells express somatostatin and localize to the hilar region [26,27]. We used PKMζ, the only known marker for late-LTP maintenance, to test the possibility that CCT increases MPP synaptic plasticity onto a somatostatin-expressing (SST+) cell population. We chose PKMζ because acquiring active place avoidance memory enhances and alters long-term plasticity at Schaffer collateral synapses [6] and increases *de novo* PKMζ hippocampal expression for at least 1 month [10,11], and requires persistent activation of the kinase [9,28], that is both necessary and sufficient for maintaining late-LTP [29]. One week after CCT but not after SE training, DG PKMζ immunostaining was increased relative to task-naïve Gad2Cre-ChR2eYFP mice, especially at the supraDG margins of the hilus (Fig. 4A) that is enriched with Gad2+ cells expressing eYFP (Fig. 4S1). CCT specifically increases PKMζ immunolabeling in hilar SST+ cells but not parvalbumin-expressing (PV+) cells (Figs. 4B, 4S2). A preferential recruitment of SST+ cells was also reported in barrel cortex after somatosensory training [30].

A neocortical-hippocampal subcircuit tuned by cognitive training

We find that CCT results in learning to learn that generalizes to another task (Fig. 1), resembling the outcome of effective CBT, and that in the awake subject, CCT attenuates the overall synaptic response to MPP stimulation at the supraDG but not infraDG (Fig. 2). The CCT-induced circuit modification includes increased MPP-supraDG synaptic efficacy, coincident with persistently increased PKMζ expression and local MMP-evoked disinhibition of the response that is coincident with increased PKMζ expression in SST+ interneurons (Figs. 3,4), known to mediate disinhibition [31]. These functional subcircuit changes are accompanied by upregulation

of PKMζ persisting at least a week in SST+ cells, that may be HIPP cells that can mediate both widespread inhibition of granule cells and local excitation of granule cells via plastic disinhibition of inhibitory neurons such as MOPP (molecular layer perforant path projecting) cells, but this has not been investigated [24,25]. These identified subcircuit changes can in principle mediate a nontopographic Mexican-hat input-controlled excitation-inhibition coordination for canonically increasing the signal-to-noise ratio and stimulus-induced representational switching in this neocortical-hippocampal circuit (Fig. 4S3) as well as stabilize the connection's input-output relationship [32,33]. Because this excitation-inhibition coordination depends only on MPP activation, it provides a distinct mechanism of DG excitation-inhibition coordination, complementary to that provided by immature adult-born granule cells that mediate mGluR-dependent inhibition in response to LPP activation and NMDAR-dependent excitation in response to MPP activation [34]. Similar disinhibitory plasticity has also been described at the Schaffer collateral and other cortical synapses [35-37]. These CCT-induced subcircuit changes have widespread effects because we detected them in field potential recordings, indicating they are not the sparse changes that mediate content-specific memory formation according to the synaptic plasticity and memory hypothesis [38]. Indeed, the functional changes we identified are more consistent with the related concepts of learning to learn, learning set and memory schema, and may explain how pretraining resulting in learning to learn can preclude the necessity for N-methyl-D-aspartate-receptor dependent LTP in the "upstairs-downstairs" and related experiments that have perplexed the neurobiology of learning and memory field [39-41]. As such, the present findings demonstrate a potential challenge to interpreting animal studies that are designed to investigate the neurobiological changes that underlie content-specific memory, because neurobiological changes that mediate generalized process memory impacting information processing, can overlap with the neurobiological changes that mediate the content-specific memory information storage itself. As demonstrated here, the same molecular and

perhaps circuit mechanisms may be engaged in different ways for process and content-specific memory.

The CCT-induced, persistent changes in neocortical-hippocampus circuit function demonstrate that appropriately structured cognitive experiences can persistently change information processing neural subcircuits. As such, the present findings strongly support the CBT-neuroplasticity hypothesis, although of course CCT likely causes additional changes that remain to be discovered. Prior work showed that preemptive CCT in adolescence prevented cognitive impairment due to neonatal neurodevelopmental brain damage [15], and as also demonstrated here, CCT was effective but mere place learning in a similar environment and task was not sufficient for these changes. This highlights the importance of cognitive control training itself, and potentially how the practice of successfully ignoring salient distracting information can have widespread CBT-like effects. The findings also demonstrate that common neurobiological mechanisms underlie the traditionally separate fields of studying schema in cognitive psychology, CBT in psychotherapy, and learned information processing in neurobiology.

REFERENCES

1 Bartlett, F. C. *Remembering: A Study in Experimental and Social Psychology*. (Cambridge University Press, 1932).

2 Harlow, H. F. The formation of learning sets. *Psychol Rev* **56**, 51-65 (1949).

3 Yeager, D. S. *et al.* A national experiment reveals where a growth mindset improves achievement. *Nature*, doi:10.1038/s41586-019-1466-y (2019).

4 Froemke, R. C. *et al.* Long-term modification of cortical synapses improves sensory perception. *Nat Neurosci* **16**, 79-88, doi:10.1038/nn.3274 (2013).

5 de Villers-Sidani, E. *et al.* Recovery of functional and structural age-related changes in the rat primary auditory cortex with operant training. *Proc Natl Acad Sci U S A* **107**, 13900-13905, doi:10.1073/pnas.1007885107 (2010).

6 Pavlowsky, A., Wallace, E., Fenton, A. A. & Alarcon, J. M. Persistent modifications of hippocampal synaptic function during remote spatial memory. *Neurobiol Learn Mem* **138**, 182-197, doi:10.1016/j.nlm.2016.08.015 (2017).

7 Cimadevilla, J. M., Fenton, A. A. & Bures, J. Functional inactivation of dorsal hippocampus impairs active place avoidance in rats. *Neurosci Lett* **285**, 53-56, doi:S0304-3940(00)01019-3 [pii] (2000).

8 Cimadevilla, J. M., Wesierska, M., Fenton, A. A. & Bures, J. Inactivating one hippocampus impairs avoidance of a stable room-defined place during dissociation of arena cues from room cues by rotation of the arena. *Proc Natl Acad Sci U S A* **98**, 3531-3536, doi:10.1073/pnas.051628398

98/6/3531 [pii] (2001).

9 Pastalkova, E. *et al.* Storage of spatial information by the maintenance mechanism of LTP. *Science* **313**, 1141-1144, doi:313/5790/1141 [pii]

10.1126/science.1128657 (2006).

10 Tsokas, P. *et al.* Compensation for PKMzeta in long-term potentiation and spatial long-term memory in mutant mice. *Elife* **5**, doi:10.7554/eLife.14846 (2016).

11 Hsieh, C. *et al.* Persistent increased PKMzeta in long-term and remote spatial memory. *Neurobiol Learn Mem* **138**, 135-144, doi:10.1016/j.nlm.2016.07.008 (2017).

12 van Dijk, M. T. & Fenton, A. A. On How the Dentate Gyrus Contributes to Memory Discrimination. *Neuron* **98**, 832-845, doi:10.1016/j.neuron.2018.04.018 (2018).

13 Talbot, Z. N. *et al.* Normal CA1 Place Fields but Discoordinated Network Discharge in a Fmr1-Null Mouse Model of Fragile X Syndrome. *Neuron* **97**, 684-697, doi:10.1016/j.neuron.2017.12.043 (2018).

14 Dvorak, D., Radwan, B., Sparks, F. T., Talbot, Z. N. & Fenton, A. A. Control of recollection by slow gamma dominating mid-frequency gamma in hippocampus CA1. *PLoS Biol* **16**, e2003354, doi:10.1371/journal.pbio.2003354 (2018).

15 Lee, H. *et al.* Early cognitive experience prevents adult deficits in a neurodevelopmental schizophrenia model. *Neuron* **75**, 714-724, doi:S0896-6273(12)00578-8 [pii] 10.1016/j.neuron.2012.06.016 (2012).

16 Wesierska, M., Dockery, C. & Fenton, A. A. Beyond memory, navigation, and inhibition: behavioral evidence for hippocampus-dependent cognitive coordination in the rat. *J Neurosci* **25**, 2413-2419, doi:25/9/2413 [pii] 10.1523/JNEUROSCI.3962-04.2005 (2005).

17 Jezek, K. *et al.* Stress-Induced Out-of-Context Activation of Memory. *PLoS Biol* **8**, e1000570, doi:10.1371/journal.pbio.1000570 (2010).

18 Yasuda, M. & Mayford, M. R. CaMKII activation in the entorhinal cortex disrupts previously encoded spatial memory. *Neuron* **50**, 309-318, doi:S0896-6273(06)00261-3 [pii] 10.1016/j.neuron.2006.03.035 (2006).

19 Witter, M. P. The perforant path: projections from the entorhinal cortex to the dentate gyrus. *Prog Brain Res* **163**, 43-61, doi:S0079-6123(07)63003-9 [pii] 10.1016/S0079-6123(07)63003-9 (2007).

20 Bragin, A., Jando, G., Nadasdy, Z., van Landeghem, M. & Buzsaki, G. Dentate EEG spikes and associated interneuronal population bursts in the hippocampal hilar region of the rat. *J Neurophysiol* **73**, 1691-1705 (1995).

21 O'Reilly, K. C., Perica, M. I. & Fenton, A. A. Synaptic plasticity/dysplasticity, process memory and item memory in rodent models of mental dysfunction. *Schizophr Res*, doi:10.1016/j.schres.2018.08.025 (2019).

22 Nitz, D. & McNaughton, B. Differential modulation of CA1 and dentate gyrus interneurons during exploration of novel environments. *J Neurophysiol* **91**, 863-872, doi:10.1152/jn.00614.2003 (2004).

23 Ruediger, S. *et al.* Learning-related feedforward inhibitory connectivity growth required for memory precision. *Nature* **473**, 514-518 (2011).

24 Han, Z. S., Buhl, E. H., Lorinczi, Z. & Somogyi, P. A high degree of spatial selectivity in the axonal and dendritic domains of physiologically identified local-circuit neurons in the dentate gyrus of the rat hippocampus. *Eur J Neurosci* **5**, 395-410 (1993).

25 Li, Y. *et al.* Molecular layer perforant path-associated cells contribute to feed-forward inhibition in the adult dentate gyrus. *Proc Natl Acad Sci U S A* **110**, 9106-9111, doi:1306912110 [pii]
10.1073/pnas.1306912110 (2013).

26 Katona, I., Acsady, L. & Freund, T. F. Postsynaptic targets of somatostatin-immunoreactive interneurons in the rat hippocampus. *Neuroscience* **88**, 37-55, doi:S0306452298003029 [pii] (1999).

27 Savanthrapadian, S. *et al.* Synaptic Properties of SOM- and CCK-Expressing Cells in Dentate Gyrus Interneuron Networks. *The Journal of Neuroscience* **34**, 8197, doi:10.1523/JNEUROSCI.5433-13.2014 (2014).

28 Serrano, P. *et al.* PKMzeta maintains spatial, instrumental, and classically conditioned long-term memories. *PLoS Biol* **6**, 2698-2706, doi:08-PLBI-RA-2746 [pii]
10.1371/journal.pbio.0060318 (2008).

29 Ling, D. S. *et al.* Protein kinase Mzeta is necessary and sufficient for LTP maintenance. *Nat Neurosci* **5**, 295-296, doi:10.1038/nn829
nn829 [pii] (2002).

30 Cybulska-Klosowicz, A. *et al.* Interneurons containing somatostatin are affected by learning-induced cortical plasticity. *Neuroscience* **254**, 18-25, doi:https://doi.org/10.1016/j.neuroscience.2013.09.020 (2013).

31 Artinian, J. & Lacaille, J. C. Disinhibition in learning and memory circuits: New vistas for somatostatin interneurons and long-term synaptic plasticity. *Brain Res Bull* **141**, 20-26, doi:10.1016/j.brainresbull.2017.11.012 (2018).

32 Olypher, A. V., Klement, D. & Fenton, A. A. Cognitive disorganization in hippocampus: a physiological model of the disorganization in psychosis. *J Neurosci* **26**, 158-168, doi:26/1/158 [pii]

10.1523/JNEUROSCI.2064-05.2006 (2006).

33 Ferrante, M., Migliore, M. & Ascoli, G. A. Feed-forward inhibition as a buffer of the neuronal input-output relation. *Proc Natl Acad Sci U S A* **106**, 18004-18009, doi:10.1073/pnas.0904784106 (2009).

34 Luna, V. M. *et al.* Adult-born hippocampal neurons bidirectionally modulate entorhinal inputs into the dentate gyrus. *Science* **364**, 578-583, doi:10.1126/science.aat8789 (2019).

35 Vasuta, C. *et al.* Metaplastic Regulation of CA1 Schaffer Collateral Pathway Plasticity by Hebbian MGluR1a-Mediated Plasticity at Excitatory Synapses onto Somatostatin-Expressing Interneurons. *eNeuro* **2**, doi:10.1523/ENEURO.0051-15.2015 (2015).

36 Donato, F., Rompani, S. B. & Caroni, P. Parvalbumin-expressing basket-cell network plasticity induced by experience regulates adult learning. *Nature* **504**, 272-276, doi:10.1038/nature12866 (2013).

37 Letzkus, J. J., Wolff, S. B. & Luthi, A. Disinhibition, a Circuit Mechanism for Associative Learning and Memory. *Neuron* **88**, 264-276, doi:10.1016/j.neuron.2015.09.024 (2015).

38 Takeuchi, T., Duszkiewicz, A. J. & Morris, R. G. The synaptic plasticity and memory hypothesis: encoding, storage and persistence. *Philos Trans R Soc Lond B Biol Sci* **369**, 20130288, doi:rstb.2013.0288 [pii]

10.1098/rstb.2013.0288 (2013).

39 Saucier, D. & Cain, D. P. Spatial learning without NMDA receptor-dependent long-term potentiation. *Nature* **378**, 186-189, doi:10.1038/378186a0 (1995).

40 Otnaess, M. K., Brun, V. H., Moser, M. B. & Moser, E. I. Pretraining prevents spatial learning impairment after saturation of hippocampal long-term potentiation. *J Neurosci* **19**, RC49 (1999).

41 Bannerman, D. M., Good, M. A., Butcher, S. P., Ramsay, M. & Morris, R. G. Distinct components of spatial learning revealed by prior training and NMDA receptor blockade. *Nature* **378**, 182-186, doi:10.1038/378182a0 (1995).

42 Mercer, L. F., Jr., Remley, N. R. & Gilman, D. P. Effects of urethane on hippocampal unit activity in the rat. *Brain Res Bull* **3**, 567-570, doi:10.1016/0361-9230(78)90089-8 (1978).

43 Shirasaka, Y. & Wasterlain, C. G. The effect of urethane anesthesia on evoked potentials in dentate gyrus. *European Journal of Pharmacology* **282**, 11-17 (1995).

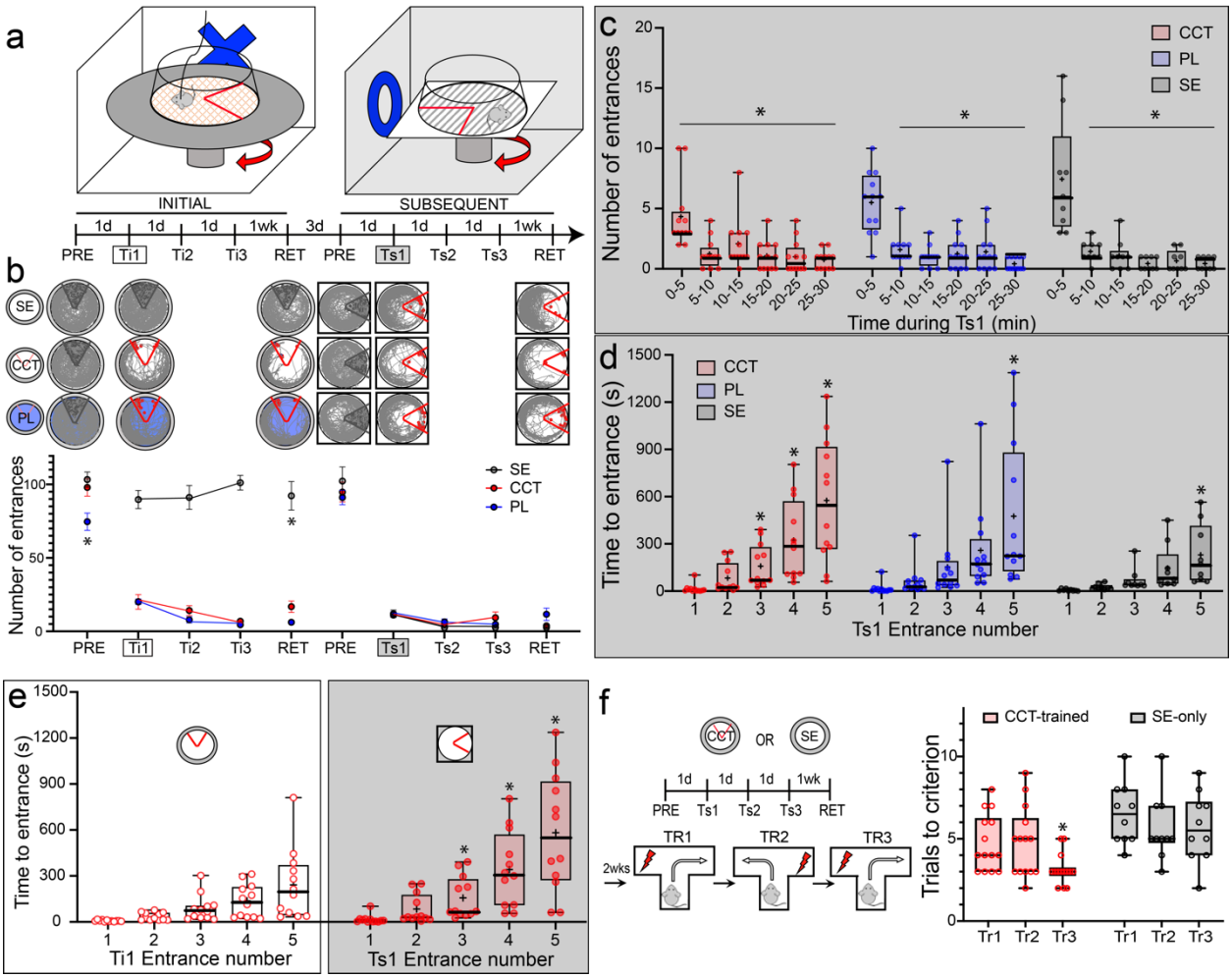

Figure 1: Learning to Learn. a) Behavioral protocol and schematic of active place avoidance in the distinct INITIAL and SUBSEQUENT training environments. After pretraining (PRE, shock off, indicated by black), mice received three daily training trials with shock on (indicated by red) in the initial (Ti) and subsequent (Ts) environments. A week later, each mouse received a retraining (RET) trial to evaluate 1-week memory. The environments were counterbalanced, and each trial was 30 min. There were 3 groups of mice: CCT (n = 12), PL controls (n= 12), and SE untrained controls (n = 9). During Initial trials, the CCT and PL controls received shock in the shock zone and the SE mice were not shocked. The arena was filled with 2 cm deep water for the PL controls to attenuate the salience of task-irrelevant olfactory cues. In the subsequent training environment, all mice received the same R+A- place avoidance training in the same conditions. b) Exemplar paths during select trials of the same representative mice, as well as

the group average performance measured by entrances into the shock zone or equivalent area for the SE mice. C,D) Group-specific box plots during the first trial in the subsequent environment (Ts1) when the avoidance response is first conditioned to the particular shock zone. c) The number of shock zone entrances during 5-min epochs is plotted as well as d) the times of the first 5 shock zone entrances. Both measures of place avoidance illustrate superior learning in the CCT group, even though they could not learn anything about the location of the current shock zone during training in the initial environment. e) Confirming that the CCT mice learned to learn R+A- active place avoidance, we compare the number of shock zone entrances during 5-min epochs of the first training trials in the initial (Ti1) and subsequent (Ts1) environments. Like Harlow (1949)[2], this illustrates, in the same mice, that there is better place avoidance during the early part of the subsequent trial compared to the initial trial, despite there being no relationship between the two environments or the shock zones. f) Learning to learn during initial CCT generalizes to L/R discrimination in a T-maze. T maze alternation in 10-trial blocks was trained 14 days after either CCT (n=14) or SE training (n=10). Performance measured as the trials to reach the criterion of the first correct responses showed the two groups were equivalent until the third block when CCT mice out performed SE mice and performed better than on the prior two blocks, even though interference was now maximal. Panels B,F: *$p < 0.05$ compared to the corresponding group measures. Panel C: *$p < 0.05$ compared to SE 0-5 min. Panels D,E: *$p < 0.05$ compared to the times of the first entrance. Panel F *$p < 0.05$ compared to all others. Box plot elements are center line: median; +: average; box limits: upper and lower quartiles; whiskers: min-max; points: all subjects.

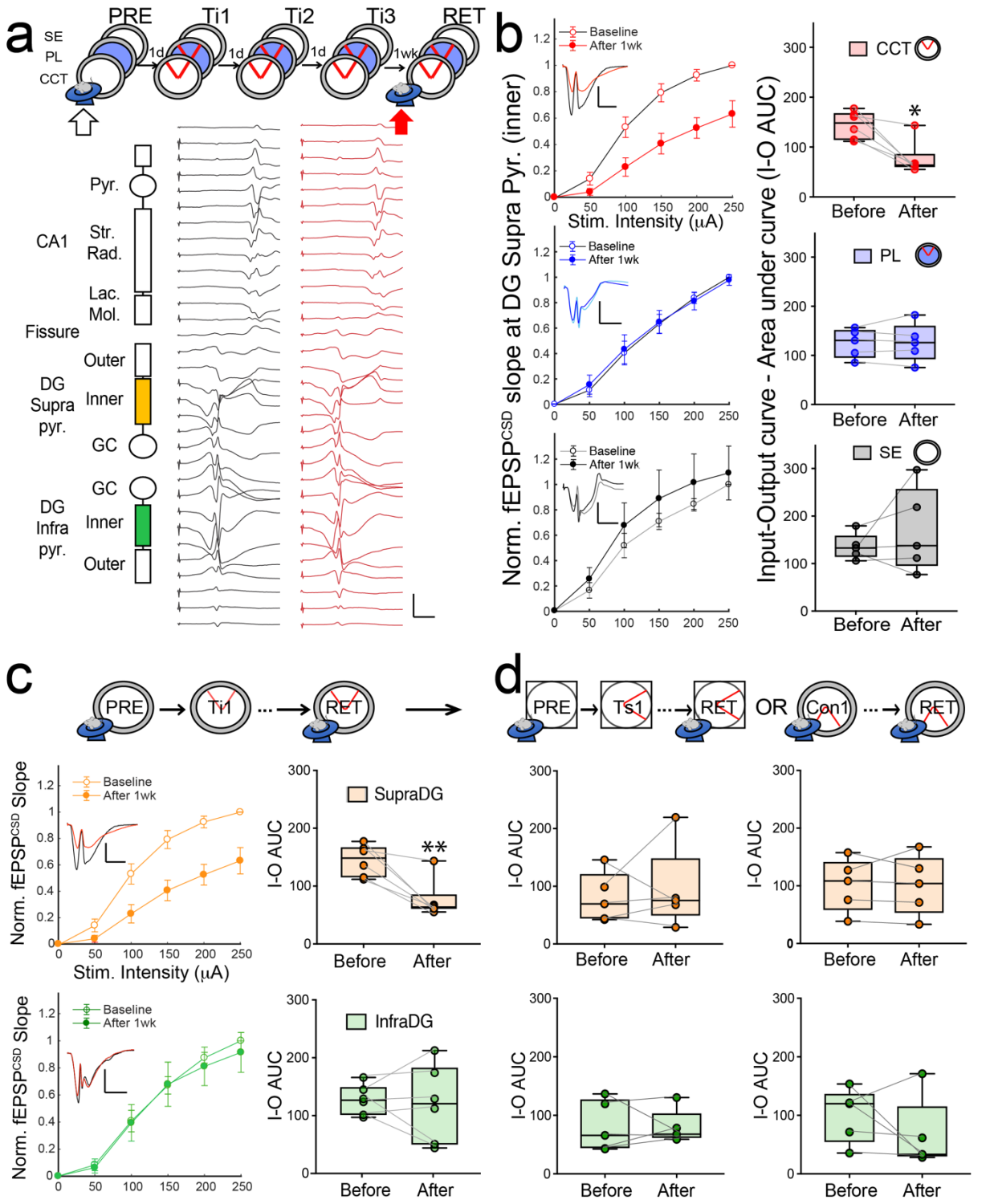

Figure 2: Cognitive control training persistently changes entorhinal-dentate circuit function. a) Experimental design and example of raw voltage trace evoked response recorded on the 32-ch linear array electrode. Schematic depicts that mice receive one of three types of

training in the same environment and before each training session evoked responses to perforant path stimulation are recorded while the mouse runs on a wheel. The voltage sources are localized to synaptic compartments along the somato-dendritic axis using current source density analyses. Scale bar: 200μA/mm^3, 5ms). b) Input-output curves showing that that CCT but not PL or SE training attenuates the supraDG population synaptic response to MPP stimulation in the inner molecular layer (Group X Training RM AVOVA, Group: $F_{2,13}$ = 1.64, p = 0.23; Training: $F_{1,13}$ = 0.88, p = 0.36; Interaction: $F_{2,13}$ = 6.36, p = 0.01; Sidak's multiple comparisons: only CCT changes circuit function *p < 0.05). (scale bar: 50μA/mm^3,5ms) c) CCT caused changes at the corresponding inner molecular layers of the supraDG (repeated from B left) but not the infraDG response to MPP stimulation (Area X Training RM ANOVA, area: $F_{1,10}$ = 0.44, p = 0.52; training: $F_{1,10}$ = 8.41, p = 0.02; interaction: $F_{1,10}$ = 5.71, p = 0.04; Sidak's multiple comparisons: only SupraDG changes circuit function **p = 0.008; supraDG was significant paired t_5 = 4.62, *p=0.006) but not in infraDG sites (paired t_5 = 0.31, p=0.76). Scale bar: 50μA/mm^3, 5ms. d) No further changes are observed in the synaptic responses after either additional CCT in a novel environment (supraDG: paired t_4 = 0.45, p=0.67; infraDG paired t_4 = 0.12, p=0.90) or in the same environment with changed shock zone (supraDG paired t_4 = 0.02, p=0.98; infraDG paired t_4 = 1.13, p=0.32). Error bars: SEM; Box plot elements are center line: median; box limits: upper and lower quartiles; whiskers: min-max; points: all subjects.

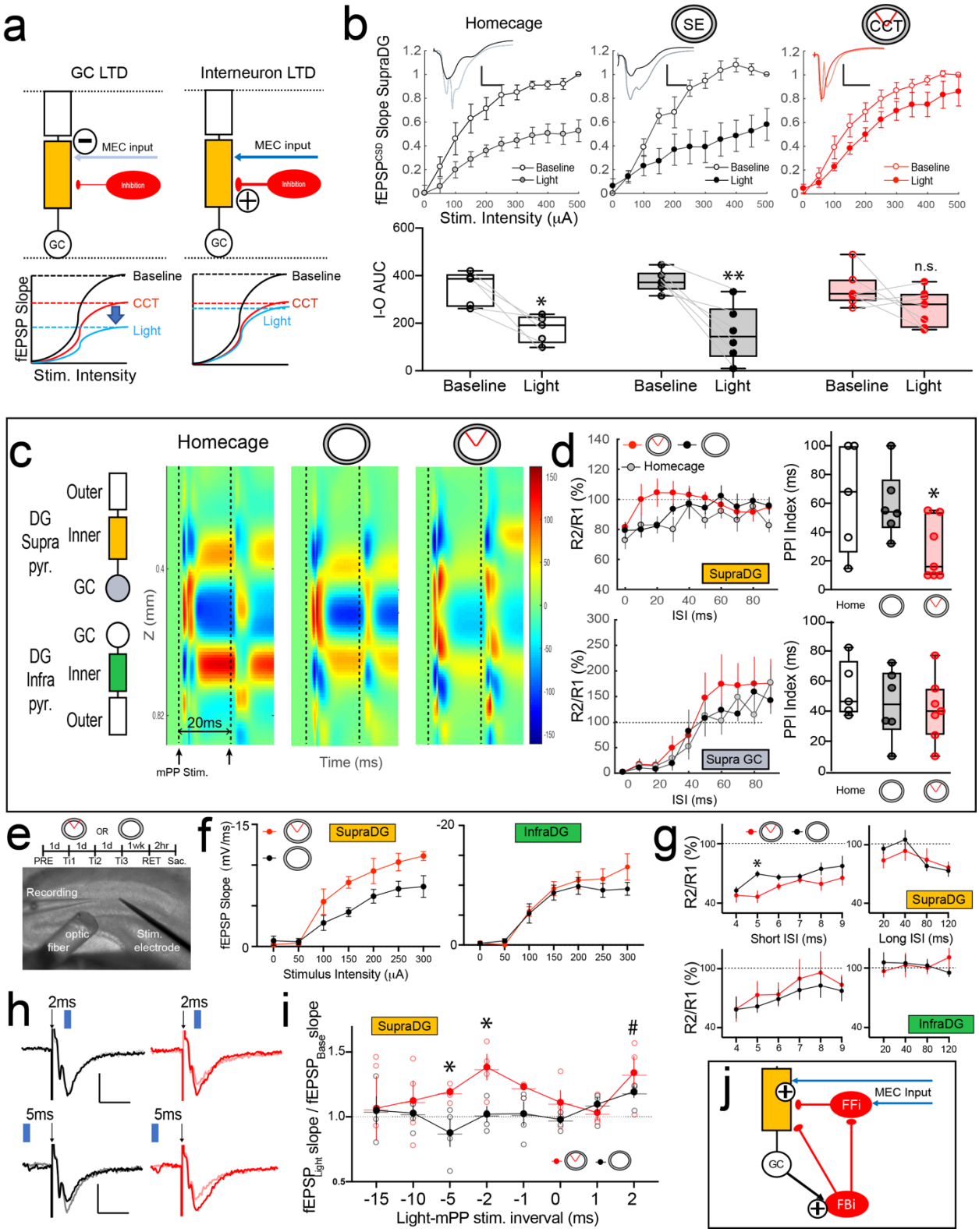

Figure 3: Cognitive control training persistently changes inhibitory entorhinal-dentate circuit function. a) Schematic of MPP→GC long-term depression (LTD) and potentiation of GC

inhibition, two hypotheses to explain the reduced DG response to MPP stimulation that is caused by CCT. b) A week after training, input-output curves (above) and their summary as the area-under-the curve (below) quantify the fEPSP at supraDG in response to MPP stimulation under urethane anesthesia, with and without concurrent light activation of ChR2 expressed in Gad2+ cells. Light-induced inhibition mimics the effect of training in home cage (paired $t_4 = 3.95$, $p<0.02$) and SE-trained (paired $t_5 = 4.77$, $p = 0.005$) control mice but the effect is occluded in CCT mice (paired $t_6 = 1.48$, $p = 0.19$). Scale bars: 100 $\mu A/mm^3$, 10ms. c) Current-source density examples of single responses to paired-pulse inhibition in homecage and SE-trained control mice and CCT mice, illustrate that MPP-stimulated inhibition is attenuated in the termination zone of supraDG after CCT. d) Summary of the training group PPI curves and indices (supraDG: $F_{2,15} = 3.90$, *p = 0.04; Granule Cell: $F_{2,15} = 0.56$, p = 0.58) e) Experimental design and photomicrograph of *ex vivo* hippocampus slices prepared 1 week after training, showing the optic fiber and recording and stimulating electrodes. fEPSP responses to stimulation of MPP terminal fibers were recorded with 1 ms light pulses to activate ChR2 in Gad2+ cells. f) supraDG and infraDG fEPSP responses to electrical MPP stimulation in slices from CCT mice. g) PPI curves in *ex vivo* hippocampus slices ($t_{10} = 3.35$, *p = 0.007). h) Exemplar responses from CCT (red) and SE-trained mice (black) with and without (baseline) 2-ms post-stimulation (above) or 5-ms pre-stimulation (below) light-activation of ChR2 in Gad2+ cells. Sale bars: 5 mV, 5 ms. i) Summary of the ratio of the fEPSP slope response measured with light stimulation normalized to the baseline response. Light activation 2 ms ($t_6 = 3.11$, *p < 0.05) and 5 ms ($t_6 = 2.83$, *p = 0.05) before MPP stimulation caused increased supraDG synaptic population responses. Light activation of inhibition immediately after MPP stimulation also appears to be potentiating, likely due to the extracellular contributions of ChR2 activation (paired t-test $t_7 = 4.14$, #p = 0.004). j) Schematic of hypothesized mechanism of potentiated MPP circuit changes observed in *ex vivo* slices, resulting in MPP response potentiation, increased feedback inhibition, and increased

disinhibition. Error bars: SEM; Box plot elements are center line: median; box limits: upper and lower quartiles; whiskers: min-max; points: all subjects.

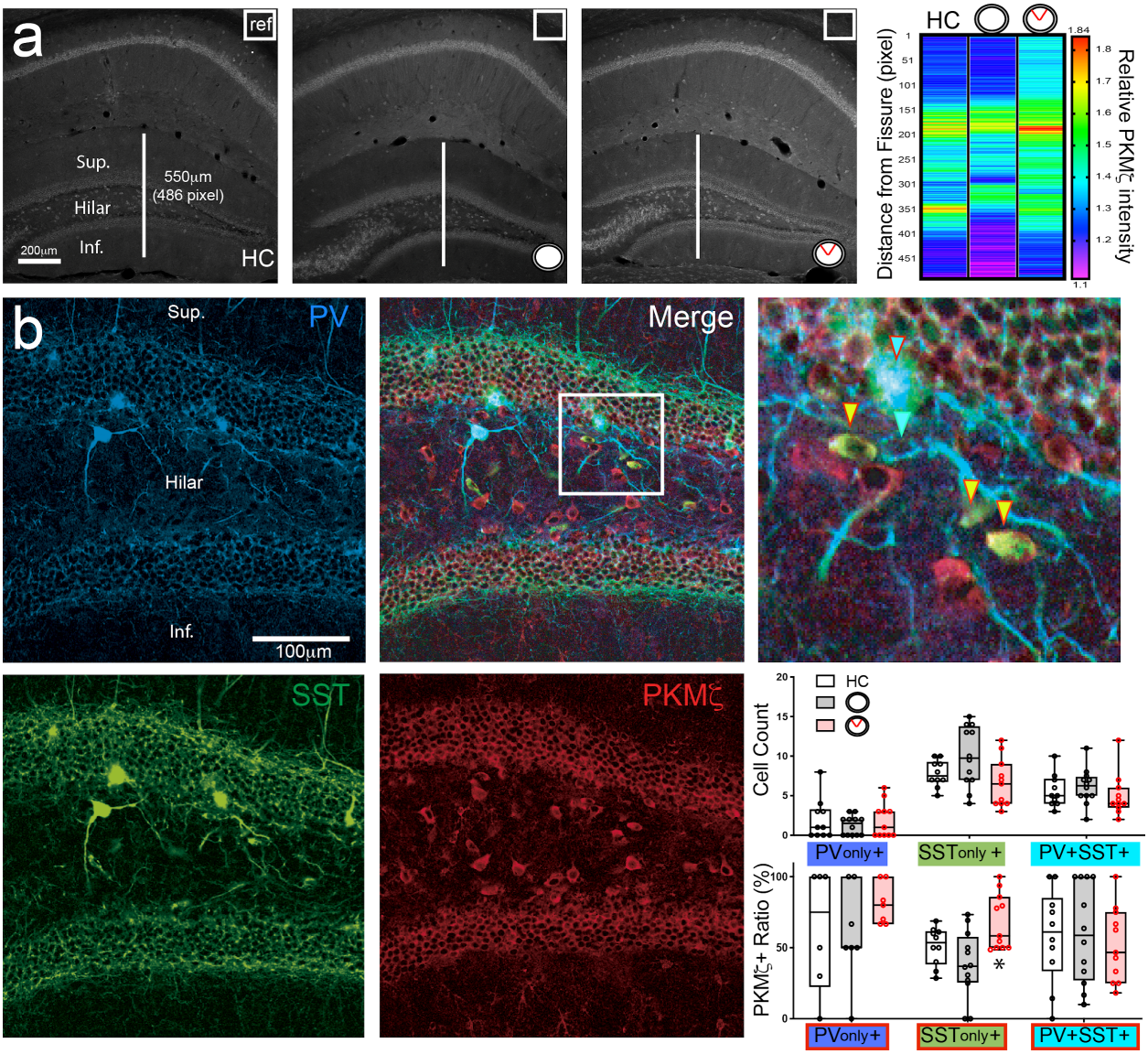

Figure 4: Cognitive control training selectively increases expression of PKMζ in somatostatin (SST)-positive cells in the suprapyramidal blade of DG. a) Anti-PKMζ immunohistochemistry illustrating PKMζ expression in dorsal hippocampus from individual mouse examples from the task-naïve homecage (left), spatial exploration (middle) and cognitive control trained (right) groups, (far right) as well as the average group expression along the DG

profile that is indicated by a white line. The color-coded average anti-PKMζ expression is relative to expression in the reference region within the same image (see white rectangles, ref.) CCT increases PKMζ expression in the dorsal suprapyramidal blade of DG. b) Example immunohistochemistry images illustrating anti-PV, anti-SST and anti-PKMζ expression in DG, as well as the corresponding quantification (right bottom). (upper) Unlike in area CA1 where PV and SST label two distinct cell classes (Fig. 4S2), PV and SST, and their co-expression define three classes of cells with differing prevalence in suprapyramidal DG that is indifferent to behavioral training. (lower) Nonetheless, CCT selectively increases PKMζ expression in the cells that exclusively express SST (SST_{only}+ Group: $F_{2,27.39} = 7.03$, $p = 0.003$; PV_{only}+ Group: $F_{2,11.06} = 0.81$, $p = 0.47$; SST+PV+ Group: $F_{2,28.33} = 0.20$, $p = 0.82$). Box plot elements are center line: median; ; box limits: upper and lower quartiles; whiskers: min-max; points: all subjects.

SUPPLEMENTARY INFORMATION

For all figures the error bars represent SEM and the box plot elements are center line: median;

+: average; box limits: upper and lower quartiles; whiskers: min-max; points: all subjects.

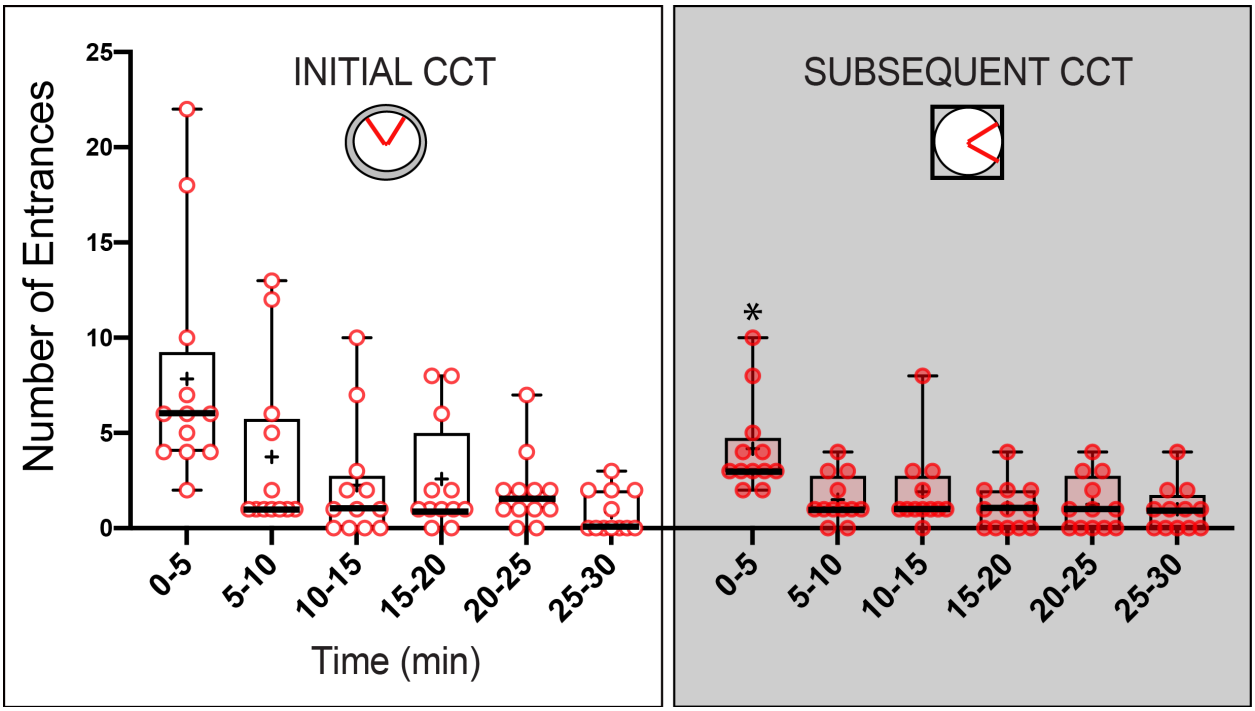

Figure 1S1 (related to Figure 1). Learning to learn. Within-session learning curve comparisons of Initial and Subsequent CCT of the same task in different environments. Although there was no discriminative spatial information in common between the two environments, mice (n = 12) acquired the subsequent conditioned-place avoidance faster than the initial place avoidance, even though the sequence of experiencing the two environments was counterbalanced. These data demonstrate learning to learn, as in the original description by Harlow (1949).

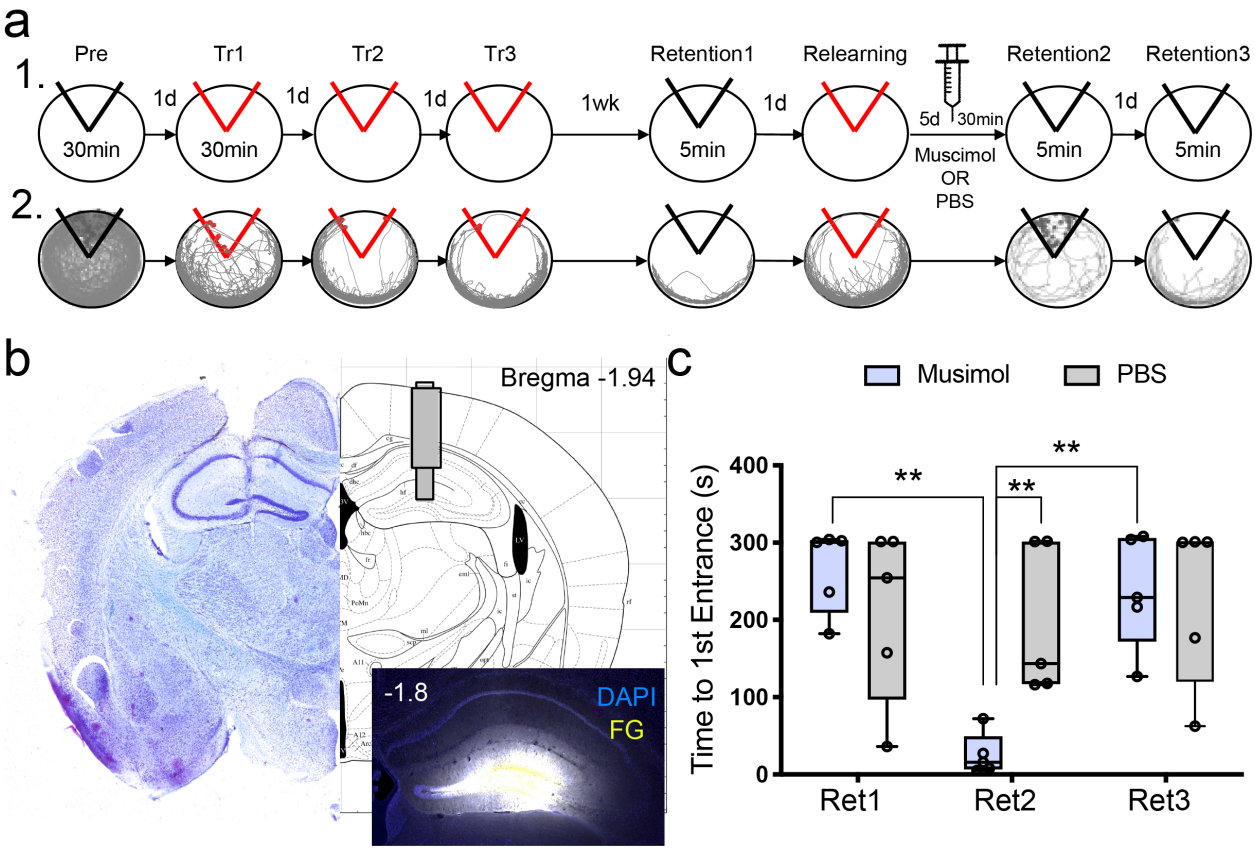

Figure 2S1 (related to Figure 2). Muscimol inactivation demonstrates DG is crucial for expression of active place avoidance several days after CCT training. a) Experimental design (1) and the tracks of an exemplar muscimol-injected mouse during each behavioral session (2). b) Schematic illustrating the injection and guide cannulae target, a histology section of the cannulation track, as well as a histological section after injecting fluorogold (FG) to estimate the infusion spread. c) A measure of memory expression illustrates that targeting muscimol at DG reversibly impairs established active place avoidance memory (Group X Retention session RM ANOVA Group: $F_{1,8} = 2.46$, $p = 0.16$; Retention session: $F_{2,16} = 5.84$, $p = 0.01$; interaction: $F_{2,16} = 4.01$, $p = 0.03$).

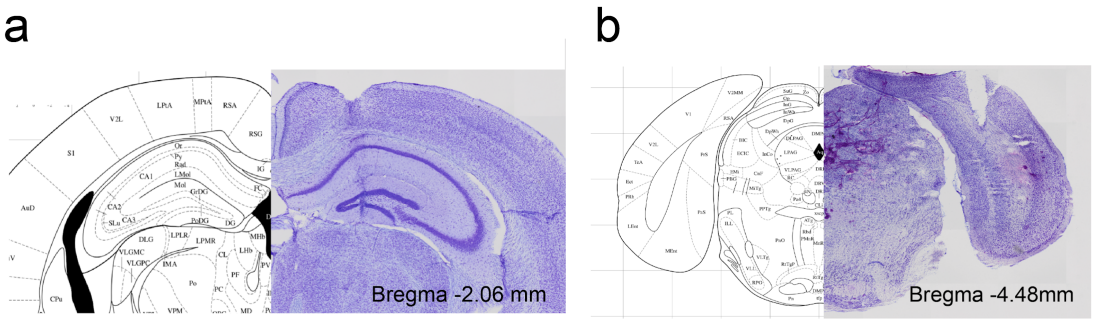

Figure 2S2 (related to Figure 2). Targeting of the recording and stimulating electrodes. Schematic and Nissl-stained histological sections form an exemplar mouse illustrating the recording and stimulation electrode sites.

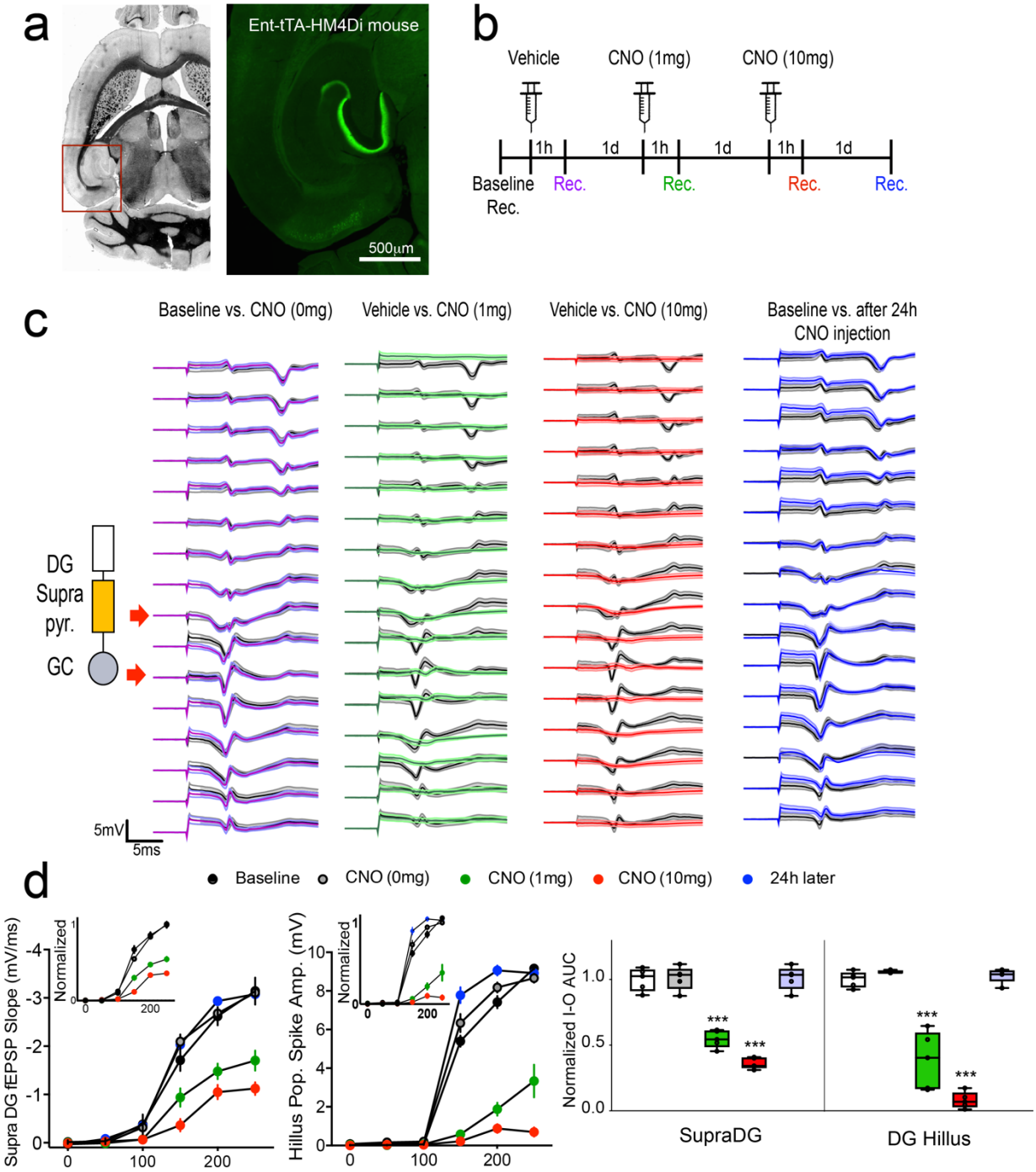

Figure 2S3 (related to Figure 2). Confirmation that electrical stimulation targeted the MPP. A) Nissl section and anti-human antigen (HA) immunostaining of transgenic mice (TRE-hM4Di-tetO+/- crossed with Ent-tTA+/-) that express the inhibitory DREADD under control of doxycycline withdrawal. The inhibitory DREADD immunoreactivity localizes to hippocampus-projecting MECII neurons. Immunofluorescence shows expression in MECII cell bodies, in the perforant path axons and in their termination zones in the molecular layer of the dentate gyrus and CA3. Expression is faint in CA1 *str. lacunosum moleculare*. Expression is in ~20% of MECII stellate cells and 5% in MECIII cells with less in adjacent regions (Kanter et al. 2017). B)

Experimental design to evaluate effective stimulation of the MPP. C) Average evoked responses recorded with a 16-site linear electrode array spanning the somato-dendritic axis of dorsal hippocampus. D) Input-output curves of fEPSP slope responses recorded from the DG molecular layer and population spike responses recorded from the DG hilus. These data quantify that responses to electrical stimulation targeted to the angular bundle is dose-dependently and reversibly suppressed by CNO-mediated activation of hM4Di in the MPP (Area X Dose RM ANOVA, Area: $F_{1,8} = 7.55$, $p = 0.02$; Dose: $F_{4,32} = 168.6$ $p = 10^{-21}$, interaction: $F_{4,32} = 5.78$, $p = 0.001$, Sidak-corrected within-area comparisons to baseline ***p<0.001).

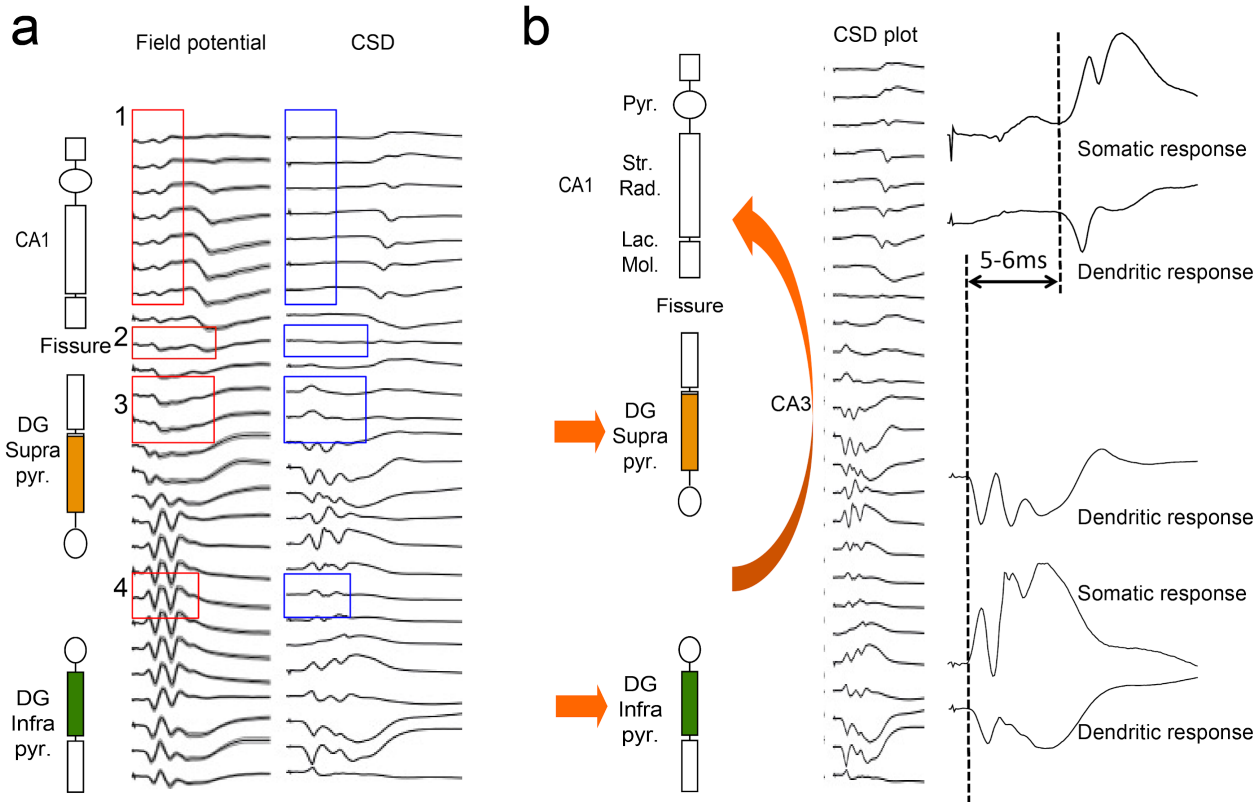

Figure 2S4 (related to Figure 2). Membrane potential vs. Current source density (CSD) plots to illustrate signal localization. a) comparison of the raw field potential (mV) plots and corresponding CSD plots along corresponding channels of the linear electrode array. Passive volume conduction strongly influences the signal recorded at adjacent electrodes in the field potential plots. Some examples are indicated by the red/blue boxes. 1: signal artifacts in CA1; 2: signal artifact at the hippocampal fissure; 3: volume conduction from MPP responses that occlude LPP responses; 4: volume conduction from the granule cell layer response occluding hilar responses. b) Representative sink and source signals and their locations from the CSD plots.

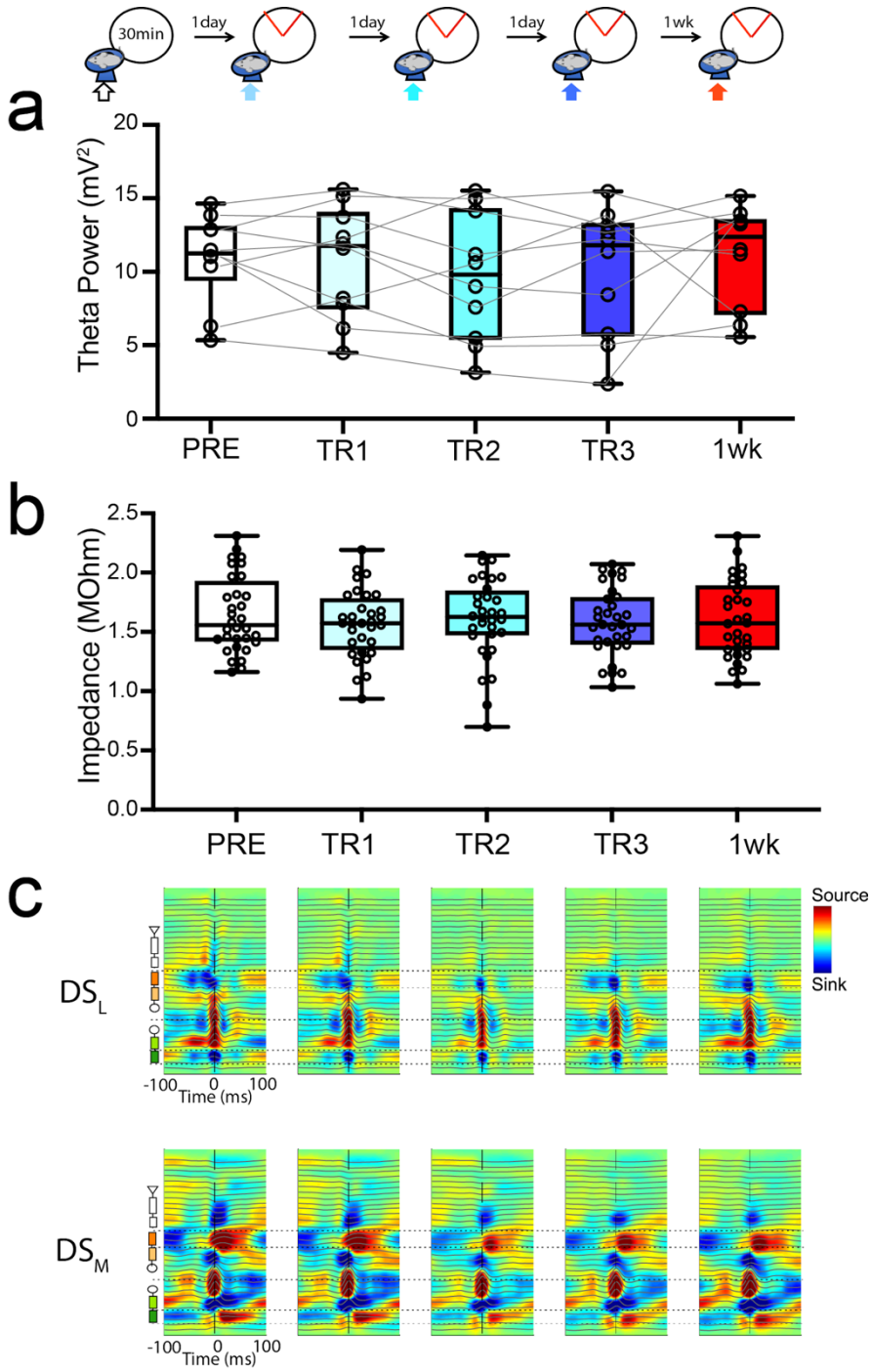

Figure 2S5 (related to Figure 2). Stability of stimulation and recording electrode properties across the duration of the experiment. a) Average power of spontaneous theta oscillations measured at the molecular-hilar region of supraDG and b) stimulation electrode impedance, both measured during wheel running before active place avoidance training (see schematic at top). Neither theta power ($F_{2.4, 21.6}$= 0.65, p = 0.55) nor electrode impedance ($F_{4,128}$= 0.294, p = 0.9) changed across the experiment, making it unlikely that changed electrode properties account for the CCT-induced differences in evoked responses. c) Session-averaged current source density (CSD) of LPP-triggered DS_L (type 1) and MPP-triggered DS_M (type2) spontaneous events also illustrate recording mechanical stability across the experiment.

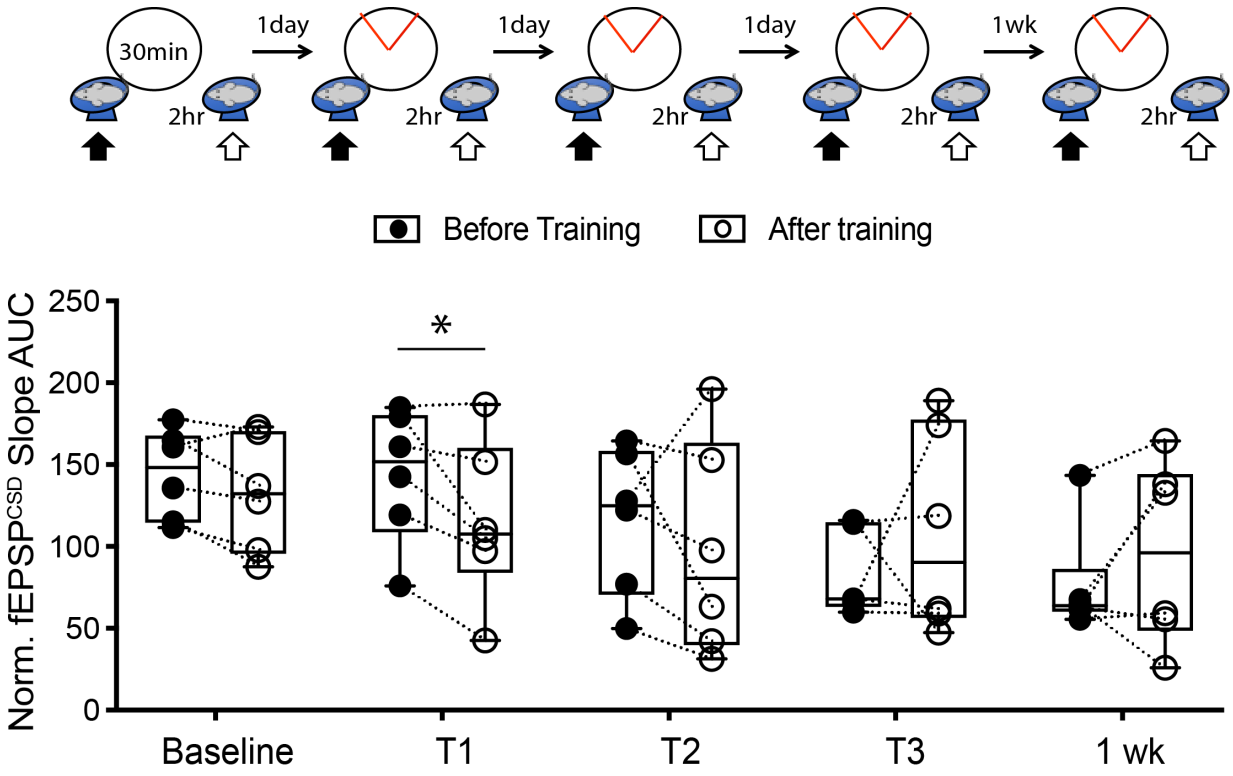

Figure 2S6 (related to Figure 2). Time course of CCT-induced changes in MPP-DG synaptic responses. fEPSP slope was normalized to the baseline slope prior to exposure to the behavioral arena. The decrease of the fEPSP response is observed within 2 hours of the first CCT trial. * indicates a significant difference from before to after a CCT trial (Paired t-test: $t_5 = 2.28$, $p = 0.04$.

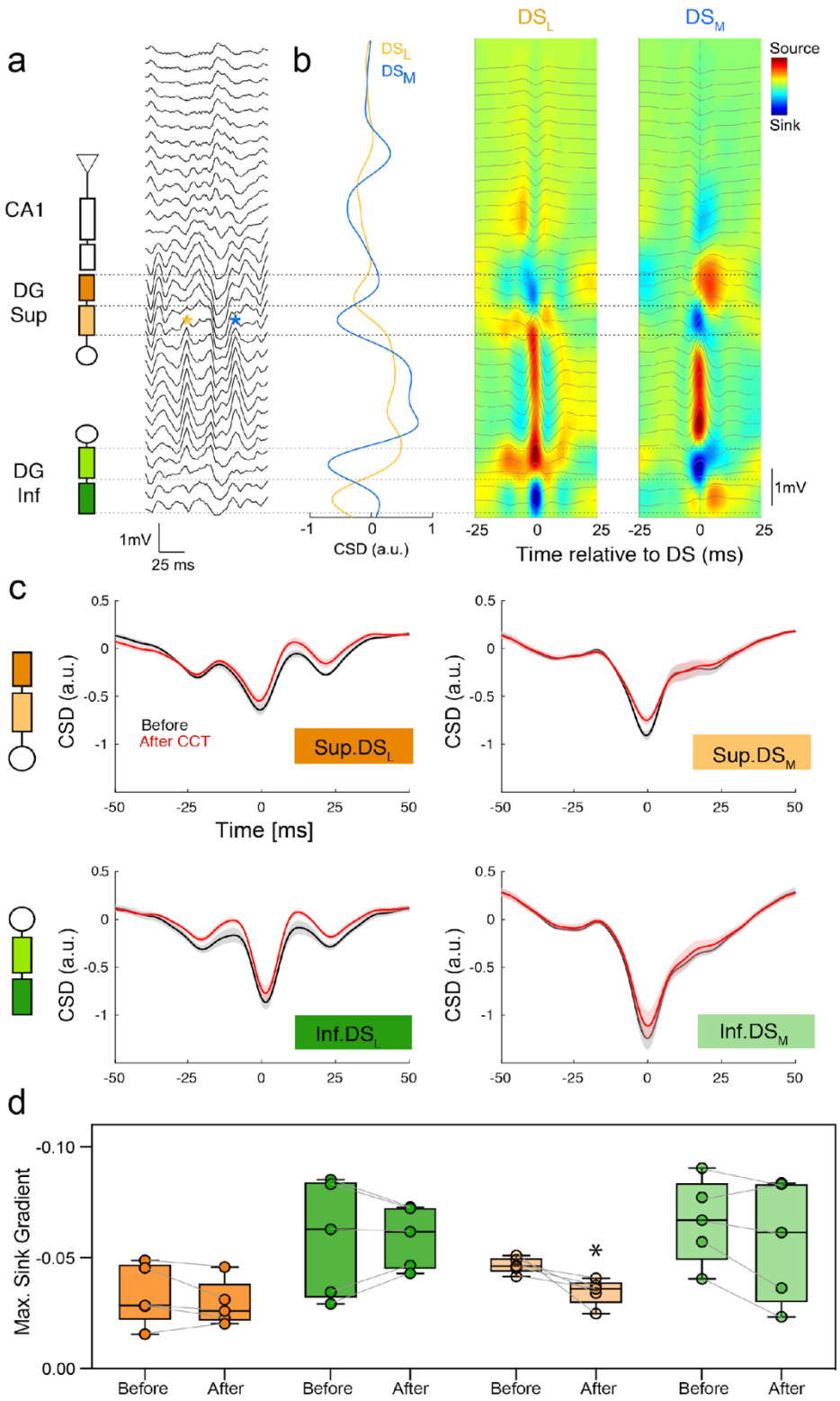

Figure 2S7 (related to Figure 2). Naturally occurring, spontaneous dentate spikes originating from MPP activation confirm the findings using evoked responses to MPP stimulation. a) A dentate spike (DS, stars) is the DG response to synchronous input from the medial and lateral perforant path, making it a physiological estimate of the MPP-DG connection that is independent of artificial stimulation. DS were identified in the DG hilus as sharp, positive waves of the local field potential with prominence (distance between peak and closest preceding or following trough) greater than 2 S.D. of all detected positive peaks, as well as width between 2.5 and 12.5 ms measured at 50% of the peak's prominence. b) Two types of dentate spikes – DS_L (type 1) and DS_M (type 2) were identified using a CSD fingerprinting method, where all DS that exhibited a symmetric pair of current sinks in the distal molecular layers of DG were identified as DS_L and DS that exhibited a symmetric pair of current sinks in the medial/proximal molecular layers of DG were identified as DS_M. The average CSD profiles of DS_L (left) and DS_M (right) computed from all classified DS events with clearly distinct pairs of current sinks in the distal and medial/proximal molecular layers of DG respectively. c) Average CSD profiles of DS-

associated current sinks in molecular layers of DG in supraDG (top row) and infraDG (bottom row) triggered by DS_L (left column) and DS_M (right column). Black and red colors represent before and after CCT training, respectively. d) Summary comparisons of maximum gradient of the DS sink (i.e. negative slope) measured before and after CCT. CCT only changed DS_M (type 2) at the supraDG site but not at the infraDG site, confirming findings assessed by stimulus evoked responses (Paired t-test: $t_4 = 3.04$, *p = 0.04).

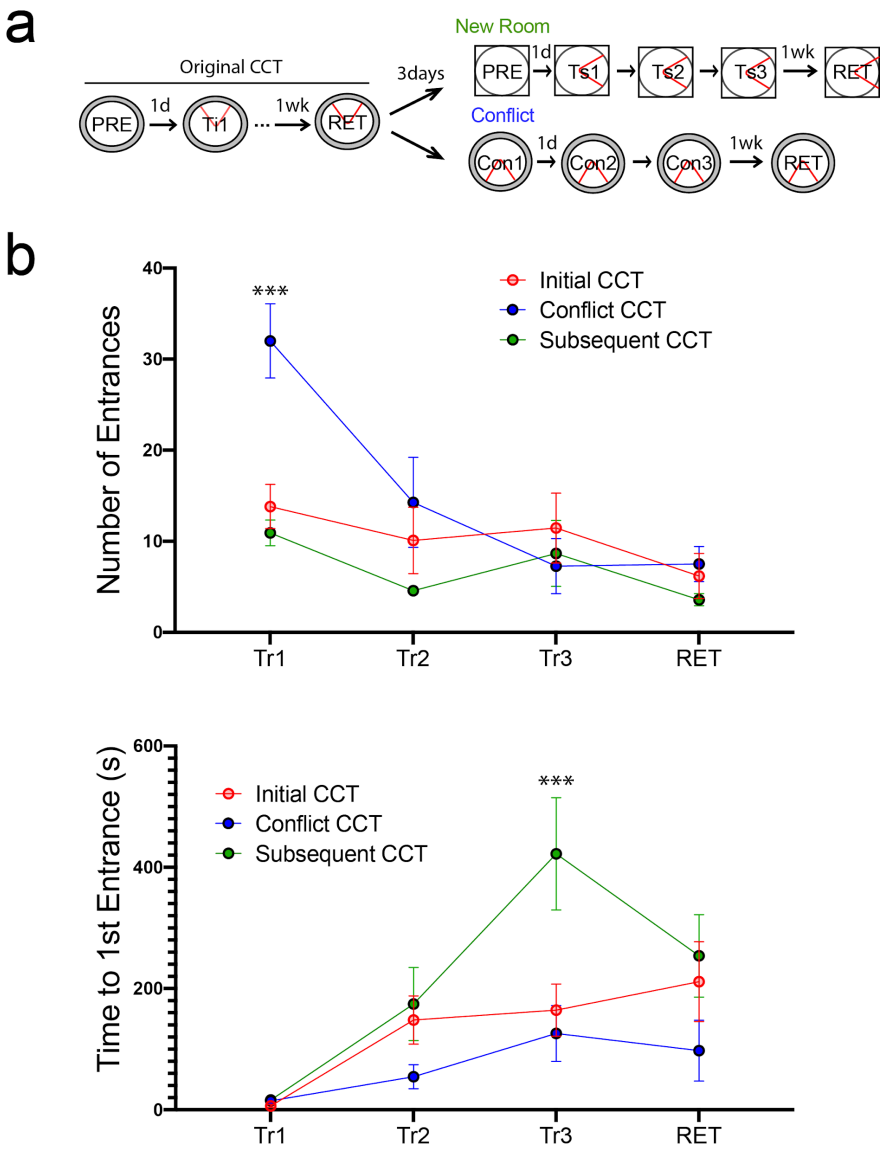

Figure 2S8 (related to Figure 2). a) Experimental design, b) Learning curves comparing initial CCT training, and subsequent CCT training to either a conflicting location of shock (Conflict CCT), or to a novel location of shock in a novel room (subsequent CCT). (Group X Trial RM ANOVA Group: $F_{2,31} = 3.95$; $p = 0.02$; Trial: $F_{2,62} = 13.53$, $p = 10^{-5}$, Interaction; $F_{4,62} = 6.28$, $p = 0.0003$).

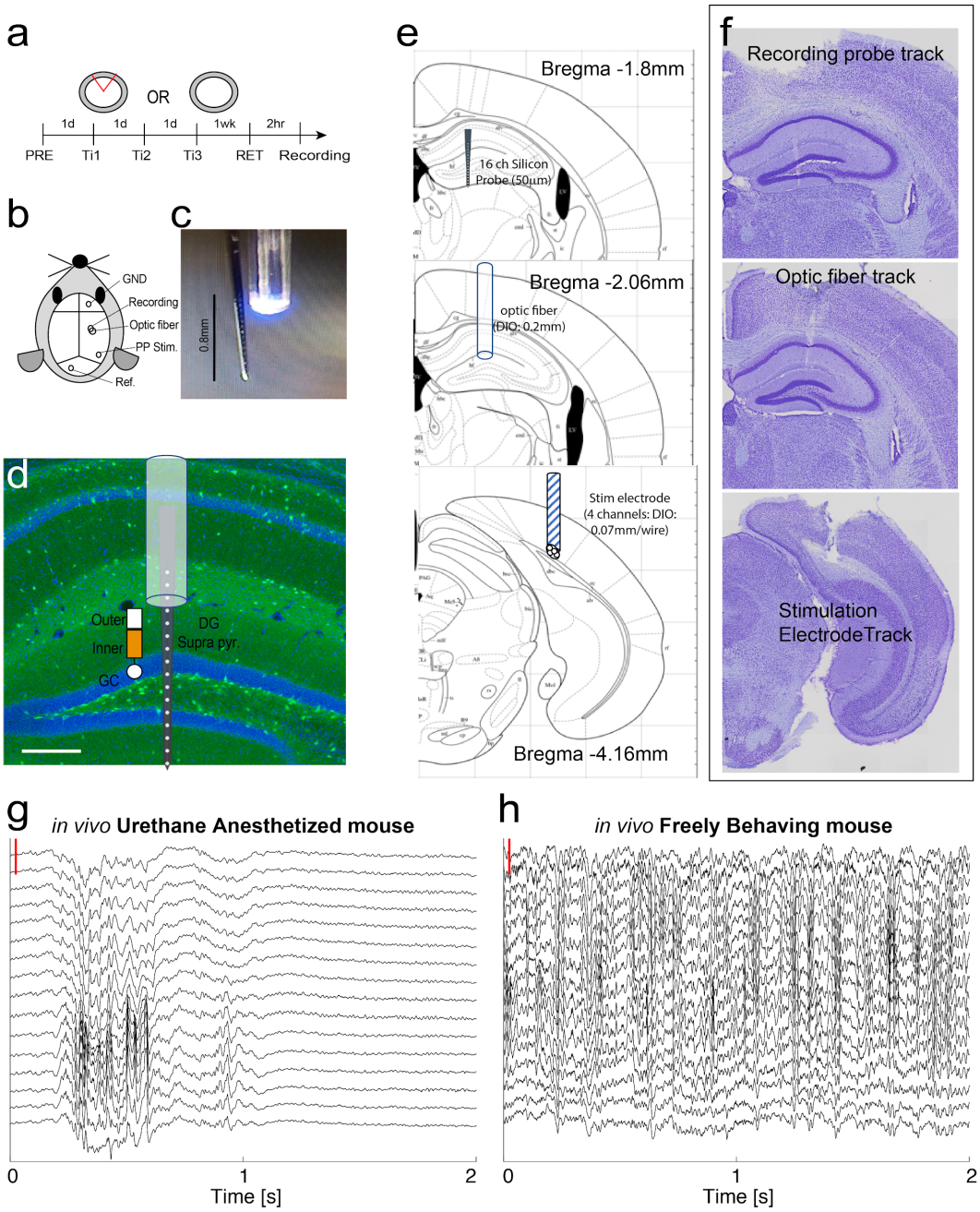

Figure 3S1 (related to Figure 3). The *in vivo* experiment under urethane anesthesia to investigate the role of inhibition in the CCT-induced effects. a) Experimental design, b) schematic of the preparation, C) photo illustrating the recording electrodes and optical stimulation, and D) The schematic is superimposed on a histological section of a Gad2-Cre-eYFP mouse's dorsal hippocampus with eYFP (green) and immunofluorescence for DAPI (blue), to indicate the circuit that was targeted (scale bar 0.02mm). E) Atlas and F) corresponding histological sections illustrating electrode and optical fiber placements. Sixteen-channel linear electrode array recordings of LFPs across the somatodendritic axis of dorsal hippocampus G) under urethane anesthesia and H) in the freely-behaving mouse. Under urethane, LFPs reflecting rhythmic ongoing synaptic activity is much attenuated compared to in the behaving mouse [42,43]. Voltage scale (red bar) = 1 mV.

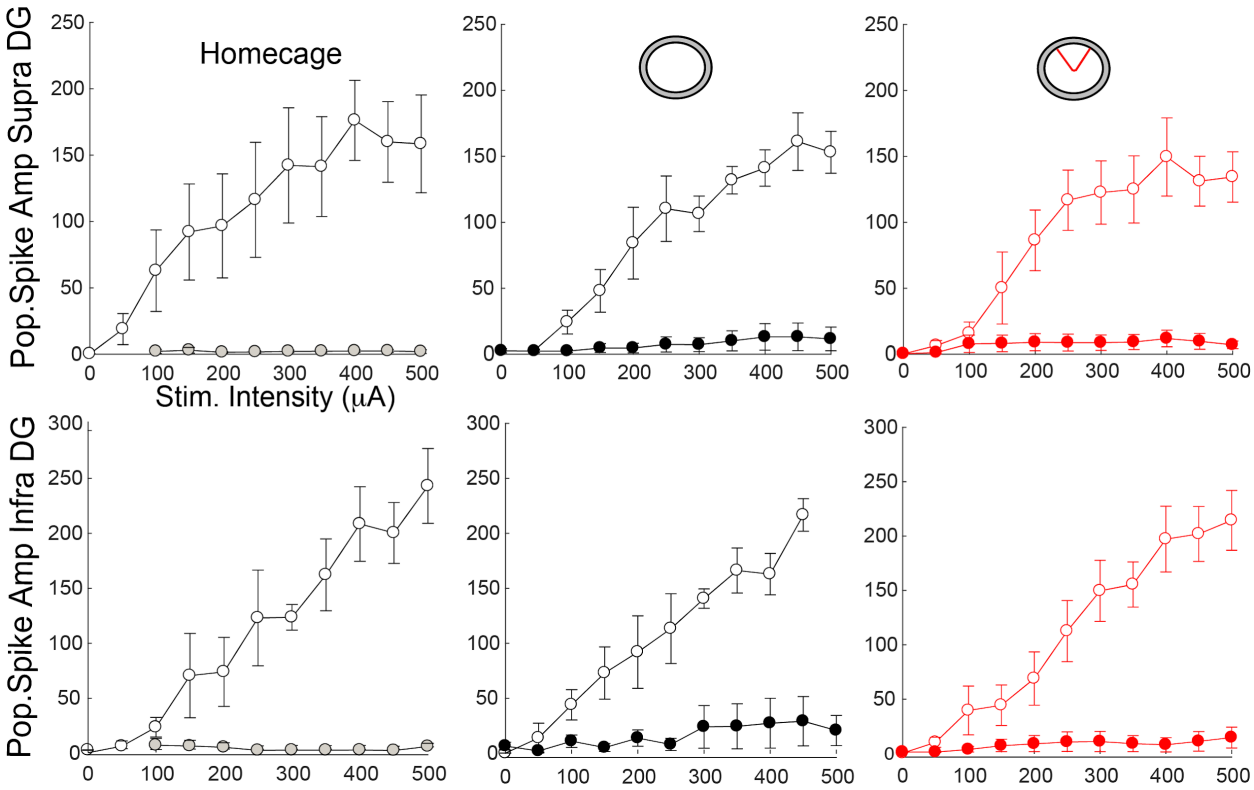

Figure 3S2 (related to Fig 3). Population spike responses are blocked by activating ChR2 in Gad2-expressing cells 5 ms before MPP stimulation *in vivo* under urethane anesthesia, regardless of prior training. This demonstrates light-triggered inhibition is effective in all groups.

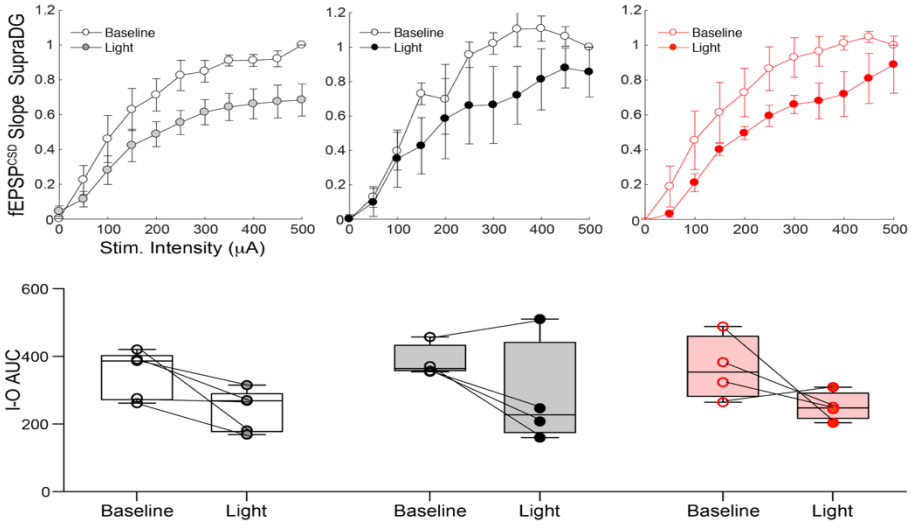

Figure 3S3 (related to Fig 3). fEPSP evoked responses at supraDG are reduced by activating Gad2-expressing cells at the same time as MPP stimulation *in vivo*, regardless of prior training. Group X Stimulation ANOVA, Group: $F_{2,10} = 0.380$, $p = 0.69$; Stimulation: $F_{1,10} = 12.15$, $p = 0.006$; interaction: $F_{2,10} = 0.007$, $p = 0.99$).

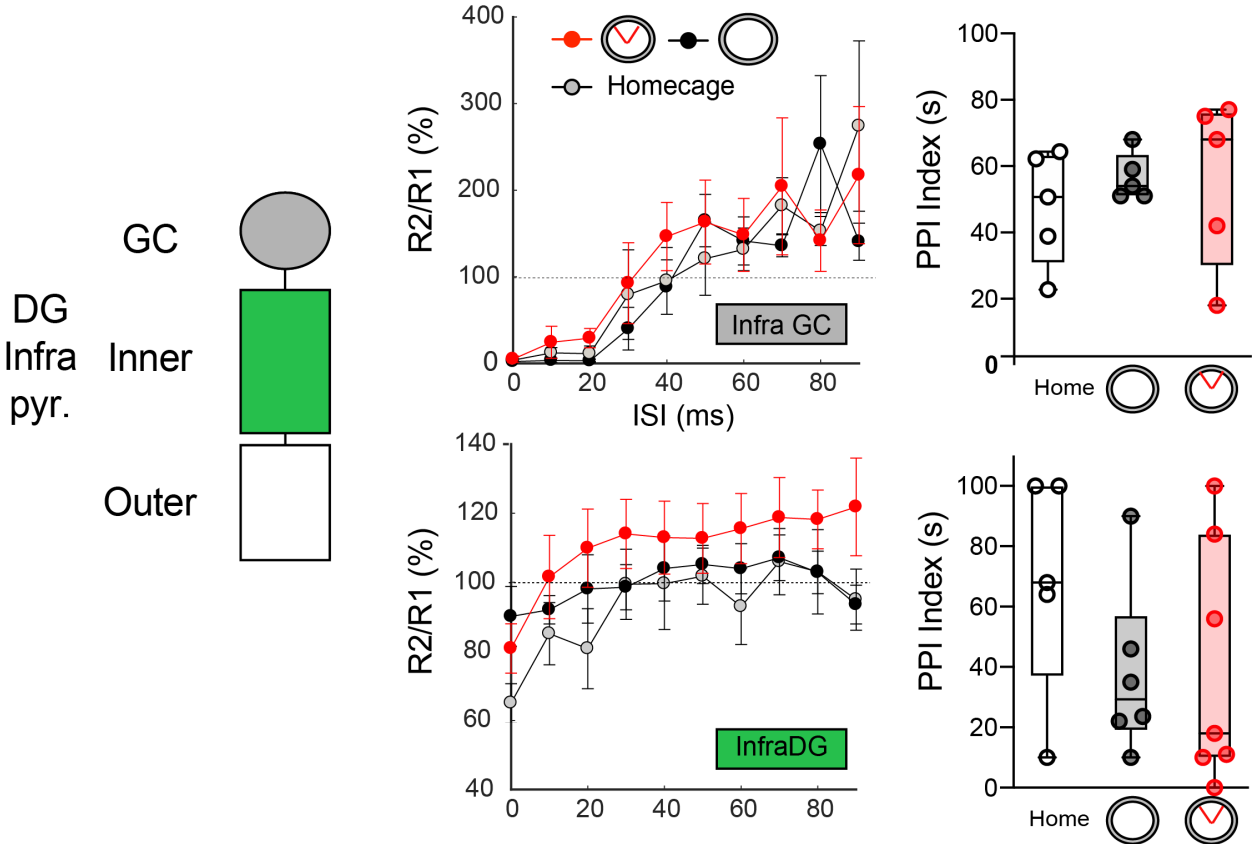

Figure 3S4 (related to Figure 3). Paired-pulse inhibition and facilitation measured at the infrapyramidal blade of DG are not changed in CCT mice. Responses to MPP stimulation were recorded in urethane-anesthetized mice at the inner molecular and granule cell layers of the infraDG. Significant changes were not detected although there is a hint of enhanced facilitation in the CCT group. (infraDG Group: $F_{2,15} = 1.24$, $p = 0.31$; Granule Cell Group: $F_{2,15} = 0.36$, $p = 0.70$)

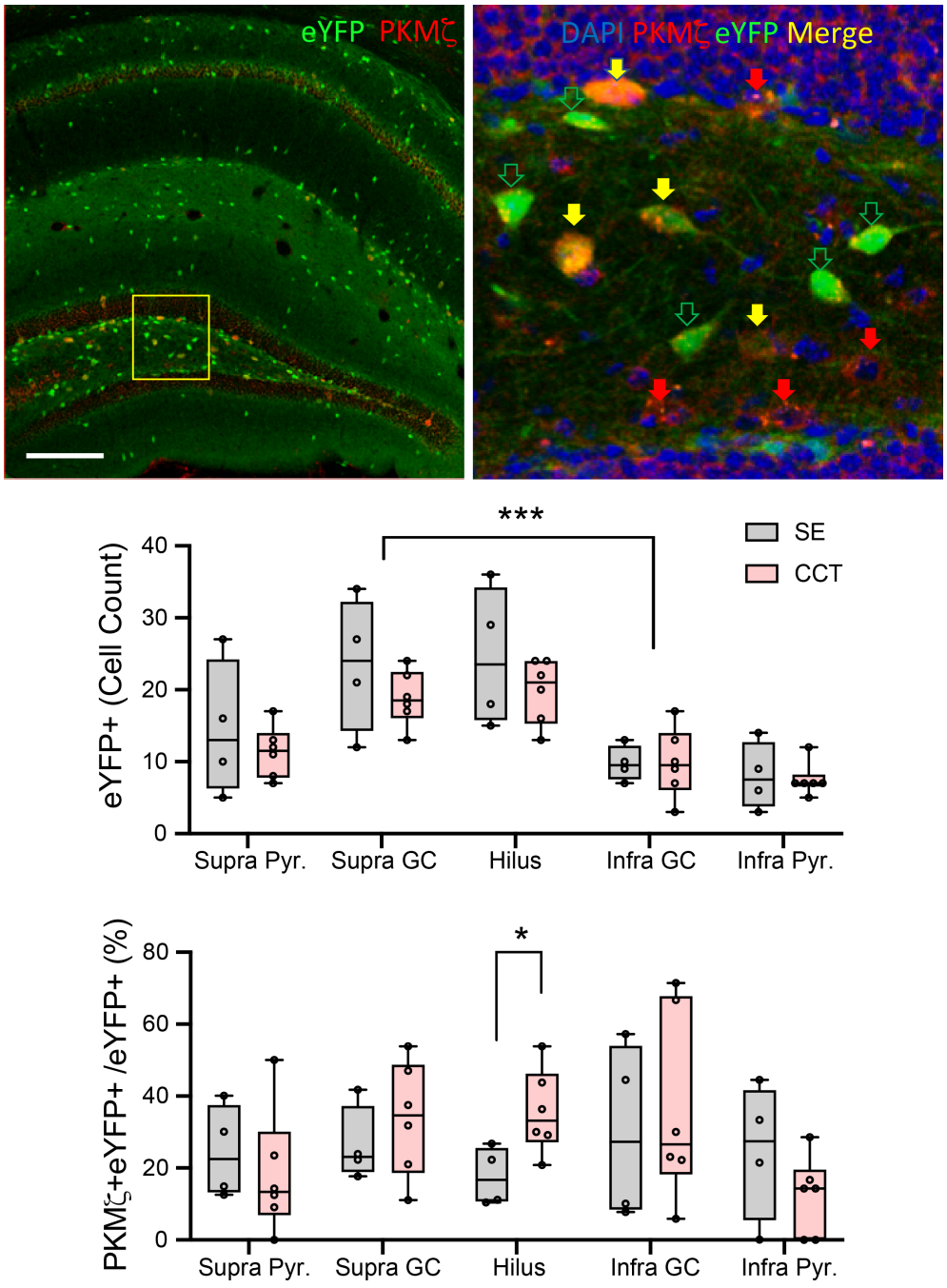

Figure 4S1 (related to Figure 4). Gad2-expressing interneurons are more abundant in supraDG and the DG hilus, where they selectively express more PKMζ in CCT mice. Immunohistochemistry for anti-eYFP labels Gad2-expressing interneurons and anti-PKMζ labels cells expressing PKMζ in Gad2Cre-ChR2eYFP mice. Top) Example immunostaining (scale bar 0.02mm); Middle) cell counts per section document enrichment of inhibitory interneurons in supraDG and hilus (t_{18} = 4.52, ***p = 0.0002). Bottom) average cell counts per section indicate enriched PKMζ expression in inhibitory neurons of the DG hilar region in mice with CCT training compared to control SE training (t_8 = 2.66, *p = 0.03).

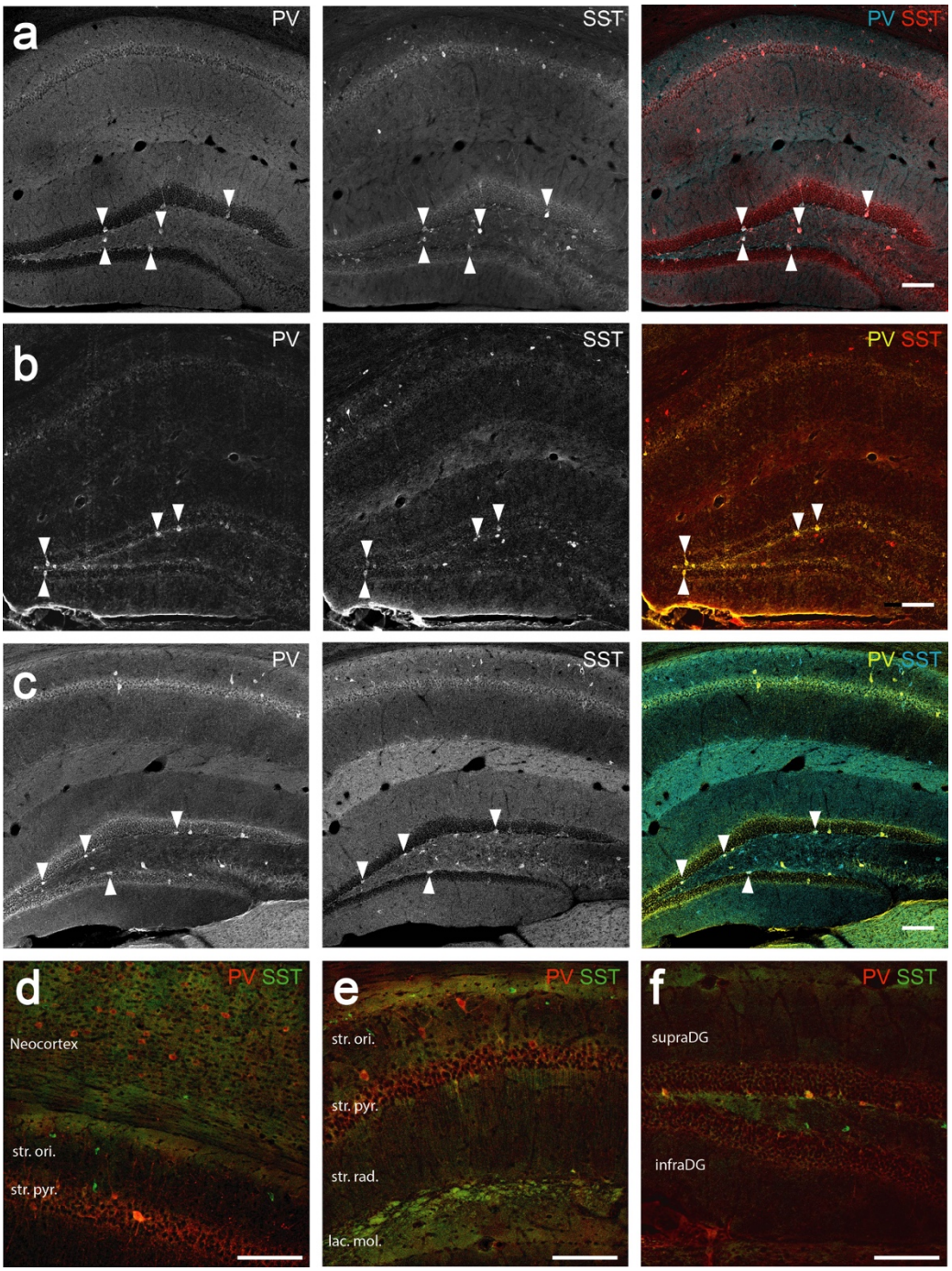

Figure 4S2 (related to Figure 4). PV and SST antibody verification tests. Immunohistochemical 10X images. scale bar: 100 µm. a) Anti-PV mouse monoclonal-anti-mouse Alexa 405, anti-SST Rat monoclonal-anti-Rat CF647 BIOTIUM. b) Anti-PV guinea pig polyclonal-anti guinea pig Alexa 568, anti-SST Rat monoclonal-anti Rat CF647. c) Anti-PV mouse monoclonal-anti-mouse Alexa 568, anti-SST Rat monoclonal-anti-Rat Alexa 405. In all cases, there is clear co-expression (white arrow) of PV and SST in DG, but no detectable colocalization of PV and SST expression is observed in CA1. Merge of Anti-PV and Anti-SST (20X images) in the same slice to illustrate lack of co-localization in d) overlying neocortex, and e) CA1 whereas PV and SST colocalize in f) dentate hilar neurons.

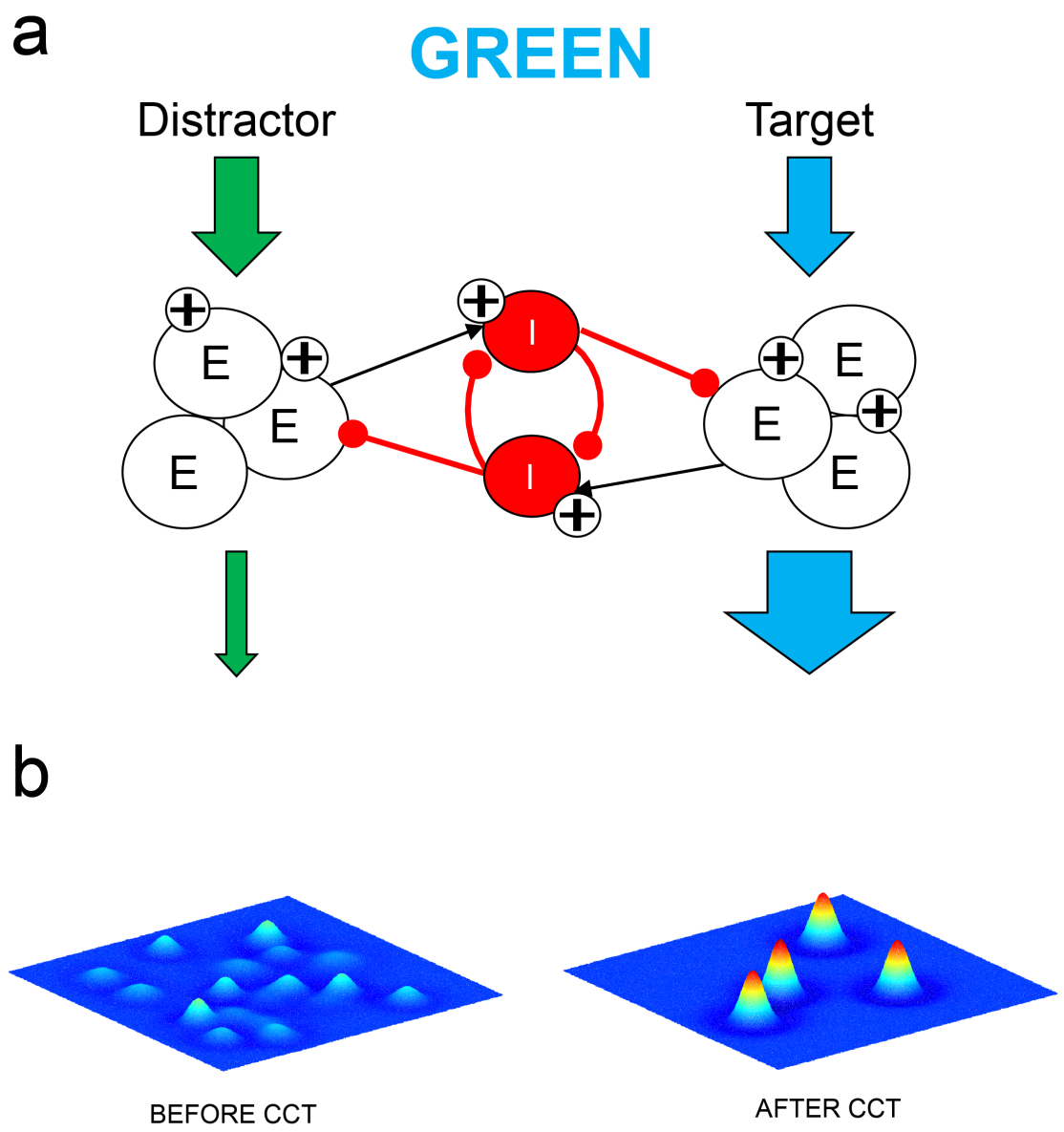

Figure 4S3. (related to Figure 4) Hypothetical excitation-inhibition coordination neural circuit changes. a) Schematic illustrating the findings that CCT causes MPP excitatory inputs to potentiate along with local activity-driven inhibition. Such neural circuit modifications organize enhanced winner-take-all competition based on excitation-inhibition coordination where afferent excitation elicits local inhibition that is demonstrated in network models to enhance signal-to-noise and switching between representational states independent of the particular information content [32]. b) Such excitation-inhibition dynamics can suppress noise and the feed-back disinhibition that CCT caused can induce what might resemble non-topographically organized Mexican-hat type excitation-inhibition coordination that is a canonical motif in winner-take all competitive networks.